

Conditional Generative Modeling of Stochastic LTI Systems: A Behavioral Approach

Jiayun Li¹ and Yilin Mo¹

Abstract—This paper presents a data-driven model for Linear Time-Invariant (LTI) stochastic systems by sampling from the conditional probability distribution of future outputs given past input-outputs and future inputs. It operates in a fully behavioral manner, relying solely on the current trajectory and pre-collected input-output data, without requiring explicit identification of system parameters. We refer to this model as a behavioral Conditional Generative Model (CGM). We prove the convergence of the distribution of samples generated by the CGM as the size of the trajectory library increases, with an explicit characterization of the convergence rate. Furthermore, we demonstrate that the gap between the asymptotic distribution of the proposed CGM and the true posterior distribution obtained by Kalman filter, which leverages the knowledge of all system parameters and all historical data, decreases exponentially with respect to the length of past samples. Finally, we integrate this generative model into predictive controllers for stochastic LTI systems. Numerical results verify the derived bounds and demonstrate the effectiveness of the controller equipped with the proposed behavioral CGM.

I. INTRODUCTION

Linear Time-Invariant (LTI) systems play a crucial role in control due to their simplicity and wide applicability in various domains, such as control design [1], [2], time-series forecasting [3], and fault detection [4], [5]. These models must be accurate, especially in demanding scenarios such as agile locomotion control [6], [7], and must account for system uncertainties for safety-critical applications [8]. Although first-principle models, i.e., models derived from physical laws, exist for many systems, they may not suffice due to factors such as deviation from the nominal parameters and/or inaccuracy in the uncertainty models [9], [10]. In contrast, input-output (I/O) data of the system are often readily available, which has recently spurred significant research into the data-driven construction of precise predictive models for unknown LTI systems [9].

Classic data-driven modeling approaches primarily use data to identify parameters of parametric models, i.e., state-space models and transfer functions [11–14]. Recently, *behavioral models*, a subset of nonparametric models, have emerged as a viable alternative to parametric models for LTI systems [9], [15–18]. Unlike system identification, which requires selecting a model structure and estimating system parameters, behavioral approaches define dynamical systems directly as sets of trajectories [19]. These methods first construct a *trajectory library* by pre-collecting input-output data,

and during online operation, they use past samples and future inputs to predict future outputs consistent with the trajectory library, eliminating the need for explicit parametric identification. This representation-free perspective avoids model-structure selection errors [16], [19]. Moreover, unlike two-stage approaches that first identify a parametric model and then design a controller, behavioral models support a direct data-to-controller design, which mitigates error propagation across multi-stage procedures and simplifies implementation in practical systems [9], [16].

For *deterministic* LTI systems, the Willems’ lemma [20], a classic result in behavioral system theory, serves as an exact behavioral model. It states that any feasible trajectory of the system can be represented as a linear combination of trajectories from the trajectory library [9]. Building on this lemma, methods such as DeePC [9] further construct direct data-driven controllers by formulating an optimization problem akin to Model Predictive Control (MPC), replacing the parametric predictive models with behavioral models. These controllers are extended to noisy systems by incorporating regularization terms into the objective function [9], [10], [16], [21]. However, these regularization terms may not faithfully represent the stochastic nature of the system, since the Willems’ lemma, which these methods rely on, applies strictly to deterministic systems. This gap motivates the development of a behavioral model for *stochastic* LTI systems.

A substantial amount of recent studies in data-driven control have focused on extending Willems’ lemma to stochastic dynamical systems that takes system uncertainties into account. One research direction incorporates additive noise, in addition to inputs and outputs, into the system trajectory, enabling the Willems’ lemma to be applied for predicting future outputs and noise based on past data. Pan et al. [22], [23] leverage this extended lemma to develop direct data-driven predictive controllers for stochastic LTI systems, while Kerz et al. [24] utilize the extended lemma to construct tube-based predictive controllers. However, the extended lemma relies on disturbances in the collected trajectories, which is typically unobservable and requires additional estimation [22]. Teutsch et al. [25] address this issue for systems with bounded noise through behavior-consistent noise sampling. In a different approach, Wang et al. [18] extends the Willems’ lemma by applying it to the expectation update of the steady-state Kalman filter. However, the expectation alone does not capture the complete distribution of the system outputs, which is crucial for methods such as robust control [26].

¹Jiayun Li and Yilin Mo are with the Department of Automation and BNRist, Tsinghua University, Beijing, P.R.China. Emails: lijiayun22@mails.tsinghua.edu.cn, ylmo@tsinghua.edu.cn.

This paper proposes a behavioral CGM that extends the Willems' lemma [20] to stochastic LTI systems. The model captures the stochastic nature of LTI systems by sampling from a data-consistent conditional distribution of future outputs, given past I/O samples and future inputs. Conditional Generative Models (CGMs) have evolved from early conditional GANs [27] and conditional VAEs [28] to become fundamental tools for machine learning [29]. Multiple advanced methods are built upon CGM foundations: score-based diffusion models learn conditional score functions for iterative denoising [30], while flow matching approaches train conditional normalizing flows by regressing vector fields of conditional probability paths [31]. CGMs have also demonstrated success in diverse applications, from image generation [27], [28] to decision-making [29]. In this work, we adapt the CGM framework to stochastic LTI systems, avoiding explicit system identification while providing uncertainty quantification.

The contribution of the paper is threefold:

- We propose a behavioral CGM that generates samples from a data-consistent conditional distribution of future outputs, given past input-output data and prescribed future inputs. The model avoids explicit parametric identification while maintaining online computational efficiency.
- We establish the theoretical foundations of the proposed CGM through a two-fold convergence analysis: first proving the asymptotic convergence of generated sample distributions with explicitly quantified rates as the trajectory library size increases, and then showing that this asymptotic distribution exponentially approaches the optimal Kalman filter prediction as the length of historical data grows.
- We develop a stochastic predictive controller based on the proposed generative modeling framework. Numerical results show that the controller achieves reduced constraint violations and competitive control cost, while achieving data and computational efficiency.

Paper Structure: In Section II, we formulate the problem of constructing a behavioral CGM for stochastic LTI systems. Section III proposes a behavioral CGM for stochastic LTI systems. Section IV and Section V analyze the performance of the proposed CGM for systems with Gaussian and non-Gaussian noise, respectively. In Section VI, we incorporate the proposed model into the predictive control framework. Finally, Section VII presents numerical results on a three-pulley system and Section VIII concludes the paper.

Notations: \mathbb{R} is the set of all real numbers. $\mathbb{R}^{a \times b}$ is the set of $a \times b$ real matrices. I_n denotes the n -dimensional unit matrix. $\mathbf{0}_n$ denotes an n -dimensional all-zero column vector and $\mathbf{0}_{m \times n}$ represents an $m \times n$ zero matrix. $\mathbf{1}_n$ and $\mathbf{1}_{m \times n}$ are similarly defined. A^\top denotes the matrix transpose. $\|A\|_2$ denotes the 2-norm for a vector A or a matrix A . For Hermitian matrices $A \in \mathbb{C}^{n \times n}$, $A \succeq 0$ implies that A is positive semi-definite. The extended expectation $\bar{\mathbb{E}}$ is defined as $\bar{\mathbb{E}}_t(\phi_t) = \lim_{t \rightarrow \infty} \mathbb{E}(\phi_t)$ for an appropriate ϕ .

Following control theory conventions, all lowercase variables with time subscripts (x_t, y_t, u_t, ϕ_t) represent the system's time-indexed signals. In our stochastic setting, unless otherwise specified, both these quantities and their samples are modeled as *random vectors*, which is consistent with the standard probabilistic viewpoint adopted in large-sample analyses such as the law of large numbers [32].

II. PROBLEM FORMULATION

Consider an n -dimensional LTI system with m inputs and p outputs taking the following form:

$$\begin{aligned} x_{t+1} &= Ax_t + Bu_t + w_t, \\ y_t &= Cx_t + v_t, \end{aligned} \quad (1)$$

where w_t and v_t represent i.i.d. Gaussian process and observation noise with zero mean and covariances $Q \succeq 0, R \succ 0$, respectively. Without loss of generality, we assume that (A, B, C) is a minimal realization of the system (1), which implies that the system is both controllable and observable. Let ℓ denote the lag [9] of the system. All parameters A, B, C, Q, R are treated as unknown parameters¹.

When the system (1) is noise-free, i.e., $w_t = 0, v_t = 0$, the input-output relationship of the system can be exactly represented by a behavioral model, known as the Willems' lemma [20]. Specifically, suppose we are provided with a trajectory library \mathcal{D} , an offline dataset representing the system's behavior, consisting of a single trajectory:

$$\mathcal{D} = \{\tilde{u}_t, \tilde{y}_t\}_{t=1}^K.$$

Let $\tilde{u} = \text{col}(\tilde{u}_1, \dots, \tilde{u}_K)$, $\tilde{y} = \text{col}(\tilde{y}_1, \dots, \tilde{y}_K)$. Moreover, let $\mathcal{H}_{T_{ini}+T}(\tilde{u})$ denote the following Hankel matrix formed from \tilde{u} :

$$\mathcal{H}_{T_{ini}+T}(\tilde{u}) = \begin{bmatrix} \tilde{u}_1 & \cdots & \tilde{u}_{K-T_{ini}-T+1} \\ \vdots & \ddots & \vdots \\ \tilde{u}_{T_{ini}+T} & \cdots & \tilde{u}_K \end{bmatrix},$$

and $\mathcal{H}_{T_{ini}+T}(\tilde{y})$ is similarly defined. Moreover, define

$$\begin{bmatrix} \tilde{U}_p \\ \tilde{U}_f \end{bmatrix} \triangleq \mathcal{H}_{T_{ini}+T}(\tilde{u}), \quad \begin{bmatrix} \tilde{Y}_p \\ \tilde{Y}_f \end{bmatrix} \triangleq \mathcal{H}_{T_{ini}+T}(\tilde{y}), \quad (2)$$

where \tilde{U}_p consists of the first T_{ini} block rows of $\mathcal{H}_{T_{ini}+T}(\tilde{u})$, and \tilde{U}_f consists of the last T block rows of $\mathcal{H}_{T_{ini}+T}(\tilde{u})$. \tilde{Y}_p and \tilde{Y}_f are similarly defined. The subscript p and f represents past and future trajectories respectively, and the subscript ini stands for initial.

Assumption 1 (Persistency of Excitation). *The given input-output trajectory $\{\tilde{u}_t, \tilde{y}_t\}_{t=1}^K$ has length $K \geq (m+1)(T_{ini}+T+n)-1$. Moreover, the input sequence \tilde{u} is persistently exciting of order at least $T_{ini}+T+n$, meaning that $\mathcal{H}_{T_{ini}+T+n}(\tilde{u})$ has full row rank.*

Based on the trajectory library \mathcal{D} of the noise-free system (1), consider any trajectory $\{u_t, y_t\}_{t=1}^{T_{ini}+T}$ of length

¹The value of A, B, C, Q, R are only used to characterize the performance of the proposed CGM, and are absent in the construction of the CGM.

$T_{ini} + T$ from the system. For simplicity, we assume that the current time step is T_{ini} , which allows us to separate the trajectory into past and future components:

$$\begin{aligned} u_{ini} &= \text{col}(u_1, \dots, u_{T_{ini}}), y_{ini} = \text{col}(y_1, \dots, y_{T_{ini}}), \\ u_f &= \text{col}(u_{T_{ini}+1}, \dots, u_{T_{ini}+T}), \\ y_f &= \text{col}(y_{T_{ini}+1}, \dots, y_{T_{ini}+T}). \end{aligned} \quad (3)$$

Here, u_{ini}, y_{ini} represent the past I/O samples, and u_f, y_f correspond to the future inputs and outputs of the system. Then, the Willems' lemma states the following result:

Proposition 1 (Willems' lemma [9], [20]). *Assume that the input-output data $\{\tilde{u}_t, \tilde{y}_t\}_{t=1}^K$ satisfy Assumption 1 and that $T_{ini} \geq \ell$. Let $(u_{ini}, y_{ini}, u_f, y_f)$ be any length- $(T_{ini} + T)$ input-output trajectory that is generated by the system (1). Then there exists a vector $g \in \mathbb{R}^{K-T_{ini}-T+1}$ such that*

$$\begin{bmatrix} \tilde{U}_p \\ \tilde{Y}_p \\ \tilde{U}_f \\ \tilde{Y}_f \end{bmatrix} g = \begin{bmatrix} u_{ini} \\ y_{ini} \\ u_f \\ y_f \end{bmatrix}. \quad (4)$$

Moreover, if g satisfies:

$$\begin{bmatrix} \tilde{U}_p \\ \tilde{Y}_p \\ \tilde{U}_f \end{bmatrix} g = \begin{bmatrix} u_{ini} \\ y_{ini} \\ u_f \end{bmatrix}, \quad (5)$$

then the associated future output is uniquely determined as $y_f = Y_f g$.

Proposition 1 shows that, under suitable assumptions, the future outputs y_f of a deterministic LTI system are *uniquely determined* from past inputs and outputs together with prescribed future inputs. This deterministic characterization reduces the prediction of future outputs to solving a linear equation. However, this determinism no longer holds for the stochastic system (1), since the outputs become random vectors driven by the noise processes. Hence, the value of y_f is not uniquely determined but varies across realizations, and the relevant object becomes the probability distribution of y_f given past information and future inputs.

To formalize this, we consider a probability space $(\Omega, \mathcal{G}, \mathbb{P}_u)$, where the subscript u indicates that the probability measure depends on the prescribed input sequence $\{u_t\}$. The process noise w_t and measurement noise v_t are modeled as random vectors on this space, and the outputs y_t are random vectors on $(\Omega, \mathcal{G}, \mathbb{P}_u)$ as measurable functions of the noises and the inputs.

The central object of interest is the conditional distribution

$$p_u(y_f | \mathcal{F}_{T_{ini}}^y), \quad (6)$$

where $\mathcal{F}_{T_{ini}}^y = \sigma(y_t | t \leq T_{ini})$ is the σ -algebra generated by past outputs up to time T_{ini} . For notational simplicity, and with a slight abuse of notation, we equivalently write (6) as

$$p_{sys}(y_f | \mathcal{F}_{T_{ini}}, u_f), \quad (7)$$

where $\mathcal{F}_{T_{ini}} = \sigma(u_t, y_t | t \leq T_{ini})$ includes both past inputs and outputs, and u_f are prescribed future inputs. We refer to (6)–(7) as the *true stochastic system model*.

Remark 1. *The key quantity for system modeling is the conditional distribution $p_{sys}(y_f | \mathcal{F}_{T_{ini}}, u_f)$, which characterizes how future outputs depend probabilistically on past observations and future inputs. Since this distribution is generally difficult to characterize without perfect knowledge of system parameters, the literature has proposed various approximations, including statistical moments, series-expansion coefficients, and sampled trajectories, i.e., sampling from $p_{sys}(y_f | \mathcal{F}_{T_{ini}}, u_f)$ [16], [18], [33], [34]. In this paper, we adopt the sampled-trajectory representation, as it naturally connects to many control design methods such as scenario-based MPC.*

Motivated by this viewpoint, we introduce the concept of a Conditional Generative Model (CGM). The role of a CGM is to approximate the true stochastic system model (7) by generating samples from an approximate conditional distribution q .

Definition 1 (Conditional Generative Model (CGM)). *A CGM for an LTI system is an algorithm that, given past information $\mathcal{F}_{T_{ini}}$ and prescribed future inputs u_f , generates random samples of the future output sequence*

$$\bar{y}_f \sim q(\cdot | \mathcal{F}_{T_{ini}}, u_f),$$

where q is a conditional distribution that approximates the true distribution $p_{sys}(y_f | \mathcal{F}_{T_{ini}}, u_f)$ in (7).

Note that Definition 1 formalizes a CGM at an abstract level. The assumptions on the available system information depend on the particular realization of the framework.

Ideally, when system noise is Gaussian and all system parameters (A, B, C, Q, R) are known, a Kalman filter initialized with the true initial state distribution fully characterizes the Gaussian posterior distribution $p_{sys}(y_f | \mathcal{F}_{T_{ini}}, u_f)$ through the exact mean and covariance predicted by the filter. Sampling from this Gaussian distribution yields a CGM with $q(\bar{y}_f | \mathcal{F}_{T_{ini}}, u_f) = p_{sys}(y_f | \mathcal{F}_{T_{ini}}, u_f)$, which represents the theoretical performance upper bound.

In contrast, we propose a *behavioral CGM* that requires neither prior knowledge of the system parameters nor explicit parameter identification. The only assumption is that the noise is known to be Gaussian distributed², while the system matrices (A, B, C) , the noise covariances (Q, R) , and the initial state distribution are all treated as unknown. The algorithm relies solely on pre-collected input-output trajectory data \mathcal{D} together with the current information $(u_f, \mathcal{F}_{T_{ini}})$ to predict future outputs y_f .

Compared with the ideal Kalman filter benchmark, our approximation of p_{sys} is constrained by two practical challenges: (i) the trajectory library \mathcal{D} has finite size, and (ii) only a finite past horizon (u_{ini}, y_{ini}) is available instead of the full information set $\mathcal{F}_{T_{ini}}$. These constraints induce a gap between the CGM distribution $q(\bar{y}_f | u_{ini}, y_{ini}, u_f; \mathcal{D})$ and the true stochastic system model $p_{sys}(y_f | \mathcal{F}_{T_{ini}}, u_f)$. The objective of this paper is to design a behavioral CGM

²We relax this assumption to noise with zero mean and bounded second moment in Section V.

that narrows this gap and to establish guarantees quantifying how the gap decreases with the trajectory library size and the truncation length T_{ini} .

A. Trajectory Library Construction

Before introducing the proposed behavioral CGM and analyzing its performance, we introduce additional assumptions regarding the trajectory library \mathcal{D} .

We assume that \mathcal{D} either contains *one single long trajectory* generated by system (1) or *multiple independent trajectories of the same length*. Moreover, we assume that the inputs u_t in (1) are generated by a linear controller:

Assumption 2 (Control Inputs in the Trajectory Library). *The inputs in the trajectory library are generated by the following n_{ctrl} -dimensional stabilizing controller:*

$$\begin{aligned}\phi_{t+1} &= A_{ctrl}\phi_t + B_{ctrl}y_t, \\ u_t &= C_{ctrl}\phi_t + \nu_t,\end{aligned}\quad (8)$$

where ν_t is i.i.d. Gaussian noise with zero mean and covariance $R_{ctrl} \succ 0$. We assume that the internal state ϕ_t is known and the initial state $\phi_1 \sim \mathcal{N}(0, \Sigma_\phi)$ where $\Sigma_\phi \succ 0$. We further assume that $(A_{ctrl}, B_{ctrl}, C_{ctrl})$ is a minimum realization of the controller (8) without loss of generality and (A_{ctrl}, B_{ctrl}) has controllability index κ_{ctrl} .

Remark 2. The controller described in (8) encompasses most linear control schemes with state or output feedback. For instance, white noise inputs are obtained by setting $u_t = \nu_t$. Such white noise excitation is commonly used in system identification [35–37]. PID controller can also be represented in state-space form (8) with appropriate parameter choices.

If the trajectory library consists of multiple independent trajectories, we assume, without loss of generality, that each trajectory has the same length $T_{ini} + T$, and the number of trajectories satisfies $N \geq m(T_{ini} + T) + T_{ini}p + n$. We then arrange the data into the following matrices, with each column representing a trajectory:

$$\begin{aligned}\check{U}^{(N)} &= \begin{bmatrix} \check{u}_1^{(1)} & \dots & \check{u}_1^{(N)} \\ \vdots & \ddots & \vdots \\ \check{u}_{T_{ini}+T}^{(1)} & \dots & \check{u}_{T_{ini}+T}^{(N)} \end{bmatrix}, \\ \check{Y}^{(N)} &= \begin{bmatrix} \check{y}_1^{(1)} & \dots & \check{y}_1^{(N)} \\ \vdots & \ddots & \vdots \\ \check{y}_{T_{ini}+T}^{(1)} & \dots & \check{y}_{T_{ini}+T}^{(N)} \end{bmatrix}, \\ \check{\Phi}^{(N)} &= \begin{bmatrix} \check{\phi}_1^{(1)} & \dots & \check{\phi}_1^{(N)} \end{bmatrix},\end{aligned}\quad (9)$$

where the superscript (i) indicates the i -th trajectory, and the check mark signifies that the samples are drawn from multiple independent trajectories. $\check{\Phi}^{(N)}$ consists of the first internal state of the controller in each trajectory.

Similar to the Willems' lemma, we also partition the matrices into past and future blocks by denoting the first T_{ini} block rows of $\check{U}^{(N)}$ and $\check{Y}^{(N)}$ as $\check{U}_p^{(N)}$ and $\check{Y}_p^{(N)}$, and

the last T block rows as $\check{U}_f^{(N)}$ and $\check{Y}_f^{(N)}$, respectively. For convenience, we concatenate $\check{U}_p^{(N)}, \check{Y}_p^{(N)}, \check{U}_f^{(N)}$ into a single matrix:

$$\check{Z}^{(N)} = \text{col}(\check{U}_p^{(N)}, \check{Y}_p^{(N)}, \check{U}_f^{(N)}). \quad (10)$$

The trajectory library is then denoted as:

$$\check{\mathcal{D}}^{(N)} = \{\check{\Phi}^{(N)}, \check{Z}^{(N)}, \check{Y}_f^{(N)}\}.$$

Remark 3. In the context of the closed-loop controller described in Assumption 2, incorporating the internal state ϕ_t of the controller into the trajectory library is crucial because the CGM must remove the influence of the offline controller to recover the correct conditional distribution, as demonstrated in Section IV. On the other hand, if the inputs within the trajectory library are open-loop, $\Phi^{(N)}$ can be excluded from the library.

For the single-trajectory case (as discussed in Section II), similar matrices $\tilde{U}_p, \tilde{U}_f, \tilde{Y}_p, \tilde{Y}_f$ are constructed as Hankel matrices with the assumption that the length of the trajectory $K \geq (m+1)(T_{ini}+T) + T_{ini}p + n - 1$. Next, we concatenate the internal states of the controller $\tilde{\phi}_t$ that generate the first inputs \tilde{u}_i in the i -th column of \tilde{U} into:

$$\tilde{\Phi} = [\tilde{\phi}_1 \ \dots \ \tilde{\phi}_{K-T_{ini}-T+1}]. \quad (11)$$

For simplicity of the subsequent discussions, we assume that the width of the Hankel matrices $\tilde{U}_p, \tilde{U}_f, \tilde{Y}_p, \tilde{Y}_f$ is identical to that of $\check{U}^{(N)}, \check{Y}^{(N)}$ in the multi-trajectory library $\check{\mathcal{D}}^{(N)}$, i.e.,

$$K - T_{ini} - T + 1 = N, \quad (12)$$

and denote the corresponding matrices with superscript N . Then, we concatenate $\tilde{U}_p^{(N)}, \tilde{Y}_p^{(N)}, \tilde{U}_f^{(N)}$ into a single matrix:

$$\tilde{Z}^{(N)} = \text{col}(\tilde{U}_p^{(N)}, \tilde{Y}_p^{(N)}, \tilde{U}_f^{(N)}). \quad (13)$$

Thus, the trajectory library with a single trajectory is denoted as:

$$\tilde{\mathcal{D}}^{(N)} = \{\tilde{\Phi}^{(N)}, \tilde{Z}^{(N)}, \tilde{Y}_f^{(N)}\}.$$

To unify the notation for both behavior libraries, we introduce $Z^{(N)}$ to represent either $\check{Z}^{(N)}$ or $\tilde{Z}^{(N)}$. Similarly, $\check{Y}_f^{(N)}$ and $\tilde{Y}_f^{(N)}$ are unified as $Y_f^{(N)}$, and $\check{\Phi}^{(N)}$ and $\tilde{\Phi}^{(N)}$ are unified as $\Phi^{(N)}$. Consequently, the unified notation for both behavior libraries is:

$$\mathcal{D}^{(N)} = \{\Phi^{(N)}, Z^{(N)}, Y_f^{(N)}\}, \quad (14)$$

which captures the information of the stochastic system (1).

In the following sections, based on $\mathcal{D}^{(N)}$, we propose a behavioral CGM for the stochastic LTI system (1) and analyze its performance.

III. CONDITIONAL GENERATIVE MODEL

This section presents a behavioral CGM for the stochastic LTI system (1). Specifically, consider the trajectory $(u_{ini}, y_{ini}, u_f, y_f)$ formulated in Section II. At the current time step T_{ini} , define the known *initial trajectory* as:

$$z_{T_{ini}} = \text{col}(u_{ini}, y_{ini}, u_f). \quad (15)$$

Then, to sample \bar{y}_f based on $z_{T_{ini}}$ and the trajectory library $\mathcal{D}^{(N)}$, we propose to randomly sample α from the solution set:

$$\left\{ \alpha \in \mathbb{R}^N \mid \underbrace{\begin{bmatrix} \Phi^{(N)} \\ Z^{(N)} \end{bmatrix}}_{\Xi^{(N)}} \alpha = \begin{bmatrix} 0 \\ z_{T_{ini}} \end{bmatrix} \right\}, \quad (16)$$

and the generated future outputs are:

$$\bar{y}_f = Y_f^{(N)} \alpha.$$

To sample α , we propose to decompose α into a special solution part and a general solution part:

$$\begin{aligned} \alpha = (\arg \min_g \|g\|_2^2 \mid \Xi^{(N)} g = \text{col}(0, z_{T_{ini}})) \\ + (\beta \sim \mathcal{N}(0, \frac{1}{N} I_N) \mid \Xi^{(N)} \beta = 0). \end{aligned} \quad (17)$$

The first term is the special solution that satisfies the equality constraint with minimum norm. Under Gaussian noise models, it corresponds to the maximum-likelihood estimate and serves as the deterministic baseline. The second term exploits the null space degrees of freedom to model conditional uncertainty. The Gaussian sampling is consistent with the system's noise model, while the $1/N$ variance scaling ensures that the resulting covariance converges at the correct rate as the trajectory library grows. Section IV further shows that these constructions provide asymptotically correct conditional means and covariances for the generated \bar{y}_f .

Remark 4. *Inspired by the Willems' lemma for noise-free systems, the equality constraint in the second row block of (16) ensures that the linear combination of trajectories in $\mathcal{D}^{(N)}$ matches the given initial trajectory, while the constraint $\Phi^{(N)} \alpha = 0$ eliminates the influence of offline controller states, ensuring the generated distribution reflects open-loop system dynamics rather than inconsistent information specific to the data collection phase.*

Remark 5. *We prove in Appendix IV that under Assumption 2 and when $N \geq (r+1)(T_{ini}+T) + r\kappa_{ctrl}$ with $r = n_{ctrl} + m(T_{ini}+T) + pT_{ini}$, $\Xi^{(N)}$ has full row rank almost surely. As a result, the equality constraint in (16) is feasible and both components of α in (17) are well-defined.*

Remark 6. *The special solution component in (17) is given by $\Xi^{(N)\dagger} \zeta_{T_{ini}}$. On the other hand, the random part ($\beta \sim \mathcal{N}(0, \frac{1}{N} I_N) \mid \Xi^{(N)} \beta = 0$) represents a conditional random vector. Since β is Gaussian and $\Xi^{(N)} \beta$ is a linear transformation of β , $(\beta, \Xi^{(N)} \beta)$ is jointly Gaussian. Therefore, the conditional distribution of β given $\Xi^{(N)} \beta = 0$ is well-defined and equivalent in distribution to $(I - \Xi^{(N)\dagger} \Xi^{(N)}) \beta'$, where $\beta' \sim \mathcal{N}(0, \frac{1}{N} I_N)$. As a result, the deterministic component of the CGM output is given by $\bar{y}_{f,det} = \Theta_f^{(N)} z_{T_{ini}}$, with $\Theta_f^{(N)} = Y_f^{(N)} \Xi^{(N)\dagger} \text{col}(0, I_{T_{ini}(m+p)+Tm})$, and the stochastic component is $\bar{\beta} = Y_f^{(N)} (I - \Xi^{(N)\dagger} \Xi^{(N)}) \beta'$, $\beta' \sim \mathcal{N}(0, \frac{1}{N} I_N)$.*

The procedure of the proposed CGM is summarized in Algorithm 1. In accordance with the decomposition in (17),

the algorithm consists of a deterministic minimum-norm solution consistent with the initial trajectory, and a stochastic perturbation drawn from the null space of $\Xi^{(N)}$ to represent conditional uncertainty.

Algorithm 1 Computational Procedure for Conditional Generative Model of Stochastic LTI Systems (see Remark 6 for definitions of notations such as $\Theta_f^{(N)}$ and $\bar{\beta}$).

Require: Trajectory library $\mathcal{D}^{(N)}$, initial trajectory u_{ini}, y_{ini}, u_f

- 1: Construct $\Xi^{(N)}$ according to (16) and $Y_f^{(N)}$ according to (2) for $\tilde{\mathcal{D}}^{(N)}$ or (9) for $\tilde{\mathcal{D}}^{(N)}$
- 2: $\Theta_f^{(N)} \leftarrow Y_f^{(N)} \Xi^{(N)\dagger} \text{col}(0, I_{T_{ini}(m+p)+Tm})$
- 3: $z_{T_{ini}} \leftarrow \text{col}(u_{ini}, y_{ini}, u_f)$
- 4: $\bar{y}_{f,det} \leftarrow \Theta_f^{(N)} z_{T_{ini}}$ // Deterministic prediction
- 5: Sample $\beta \sim \mathcal{N}(0, \frac{1}{N} I_N)$
- 6: $\bar{\beta} \leftarrow Y_f^{(N)} (I - \Xi^{(N)\dagger} \Xi^{(N)}) \beta$
- 7: $\bar{y}_f \leftarrow \bar{y}_{f,det} + \bar{\beta}$ // Add randomness for uncertainty
- 8: **return** \bar{y}_f

Remark 7. *To incorporate the CGM into predictive controllers, the CGM is required to generate samples online in real-time. To make this computation efficient, steps 1, 2, 5, 6 in Algorithm 1 can be performed offline, while the online computation of \bar{y}_f involves only steps 3, 4, 7. This includes a single matrix-vector multiplication $\Theta z_{T_{ini}}$ in line 4, with complexity $O(p(m+p)TT_{ini})$, and a vector addition in line 7, with complexity $O(Tp)$. Hence, the overall online computation complexity for generating T future outputs is $O(p(m+p)TT_{ini})$.*

We have proposed a behavioral CGM for the stochastic LTI system (1). In the following section, we derive theoretical guarantees on the performance of the proposed CGM.

IV. PERFORMANCE ANALYSIS

This section analyzes the performance of the proposed behavioral CGM. First, we characterize the conditional distribution of samples \bar{y}_f generated by the CGM. Then, in Section IV-A, we analyze the convergence of this distribution as the trajectory library size N increases and characterize the resulting asymptotic distribution. Finally, in Section IV-B, we assess the gap between this asymptotic distribution and the true posterior distribution generated from the Kalman filter.

Assumption 3. 1) The initial state of the current online trajectory is Gaussian distributed.

- 2a) For the multi-trajectory behavior library $\tilde{\mathcal{D}}^{(N)}$, the initial state $\tilde{x}_1^{(i)}$ of each trajectory is independently sampled from the same Gaussian distribution, $\tilde{x}_1^{(i)} \sim \mathcal{N}(0, \check{\Sigma})$, where $\check{\Sigma} \succ 0$. Moreover, we assume that $\check{\Sigma} - \check{\Sigma}_{x\phi} \check{\Sigma}_{\phi}^\dagger \check{\Sigma}_{x\phi}^\top \succ 0$, where $\check{\Sigma}_{x\phi} = \mathbb{E}(\tilde{x}_1^{(1)} \phi_1^{(1)\top})$ and Σ_ϕ is introduced in Assumption 2.
- 2b) For the single-trajectory behavior library $\tilde{\mathcal{D}}^{(N)}$, the initial state \tilde{x}_1 of the trajectory is Gaussian distributed.

The following proposition characterizes the distribution of the generated \bar{y}_f using Algorithm 1:

Proposition 2. *The conditional distribution of the generated \bar{y}_f given $z_{T_{ini}}, \mathcal{D}^{(N)}$ satisfies:*

$$\begin{aligned}\mathbb{E}(\bar{y}_f | z_{T_{ini}}; \mathcal{D}^{(N)}) &= \Theta_f^{(N)} z_{T_{ini}}, \\ \Sigma_f^{(N)} &\triangleq \text{Cov}(\bar{y}_f | z_{T_{ini}}; \mathcal{D}^{(N)}) \\ &= \frac{1}{N} Y_f^{(N)} (I - \Xi^{(N)\dagger} \Xi^{(N)}) (I - \Xi^{(N)\dagger} \Xi^{(N)})^\top Y_f^{(N)\top}.\end{aligned}\quad (18)$$

The result follows directly from Remark 6, which provides explicit expressions for both components in (17). In the following subsection, we analyze the convergence properties of both the conditional expectation coefficient $\Theta_f^{(N)}$ and the conditional covariance $\Sigma_f^{(N)}$ as trajectory library size $N \rightarrow \infty$.

A. Convergence of Conditional Distribution

In this subsection, we analyze the convergence of the distribution of the generated \bar{y}_f as N tends to infinity.

To derive the explicit form of the asymptotic distribution, we start from the ideal full-information case in which a Kalman filter (KF) has access to the true system parameters (A, B, C, Q, R) and the initial state distribution. In this setting, the KF provides the true posterior distribution of future outputs $p_{\text{sys}}(y_f | \mathcal{F}_{T_{ini}}, u_f)$ [38].

Proposition 3. *Consider the KF initialized with the true initial state distribution $x_1 \sim \mathcal{N}(\mu, P)$. Conditioned on (u_{ini}, y_{ini}, u_f) , the distribution of y_f generated by system (1) is Gaussian with mean*

$$\mathbb{E}(y_f | z_{T_{ini}}) = \eta_f(P) z_{T_{ini}} + O_f \hat{\psi}_{T_{ini}+1}^-(P) \mu, \quad (19)$$

and covariance

$$\begin{aligned}\mathcal{Y}_f(P) &\triangleq \text{Cov}(y_f | z_{T_{ini}}) \\ &= O_f P_{T_{ini}+1}^-(P) O_f^\top + G_f Q_f G_f^\top + R_f.\end{aligned}\quad (20)$$

Here, $\eta_f : \mathbb{R}^{n \times n} \rightarrow \mathbb{R}^{Tp \times (T_{ini}(m+p)+Tm)}$, $\hat{\psi}_{T_{ini}+1}^- : \mathbb{R}^{n \times n} \rightarrow \mathbb{R}^n$, and $P_{T_{ini}+1}^- : \mathbb{R}^{n \times n} \rightarrow \mathbb{R}^{n \times n}$ are linear operators that depend on the initial covariance P . The matrices O_f, G_f, Q_f, R_f are determined by the system parameters (A, B, C, Q, R) .

The proof of this proposition is provided in Appendix I.

The following theorem establishes the convergence of the conditional expectation coefficient $\Theta_f^{(N)}$ and conditional covariance $\Sigma_f^{(N)}$ from Proposition 2 to their counterparts $\eta_f(\Sigma), \mathcal{Y}_f(\Sigma)$ derived in Proposition 3 as $N \rightarrow \infty$.

Theorem 4 (Asymptotic convergence of expectation and covariance of \bar{y}_f). *Under Assumption 1-3, let $\epsilon > 0$ be arbitrary. Then, as $N \rightarrow \infty$, the coefficients in the conditional expectation and the conditional covariance of the generated*

\bar{y}_f in (18) satisfy:

$$\lim_{N \rightarrow \infty} \frac{\|\Theta_f^{(N)} - \eta_f(\Sigma)\|}{N^{-0.5+\epsilon}} = 0 \text{ a.s.}, \quad (21)$$

$$\lim_{N \rightarrow \infty} \frac{\|\Sigma_f^{(N)} - \mathcal{Y}_f(\Sigma)\|}{N^{-0.5+\epsilon}} = 0 \text{ a.s.}, \quad (22)$$

where Σ is defined as follows:

- For the multi-trajectory library $\mathcal{D}^{(N)}$,

$$\Sigma = \check{\Sigma} - \check{\Sigma}_{x\phi} \Sigma_\phi^\dagger \check{\Sigma}_{x\phi}^\top, \quad (23)$$

where Σ_ϕ is defined in Assumption 2 and $\check{\Sigma}, \check{\Sigma}_{x\phi}$ are introduced in Assumption 3.

- For the single-trajectory library $\mathcal{D}^{(N)}$,

$$\Sigma = \tilde{\Sigma}_{xx} - \tilde{\Sigma}_{x\phi} \tilde{\Sigma}_{\phi\phi}^\dagger \tilde{\Sigma}_{x\phi}^\top, \quad (24)$$

where $\tilde{\Sigma}_{xx} = \tilde{\mathbb{E}}_t(\tilde{x}_t \tilde{x}_t^\top)$, $\tilde{\Sigma}_{x\phi} = \tilde{\mathbb{E}}_t(\tilde{x}_t \tilde{\phi}_t^\top)$, $\tilde{\Sigma}_{\phi\phi} = \tilde{\mathbb{E}}_t(\tilde{\phi}_t \tilde{\phi}_t^\top)$.

The proof of this theorem is provided in Appendix II. The proof uses a martingale convergence result to establish almost-sure convergence of the sample covariance matrices, followed by a differentiability argument that preserves convergence rates.

Theorem 4 not only establishes the convergence of the conditional distribution of the generated \bar{y}_f , but also demonstrates its asymptotic equivalence to the posterior distribution of y_f generated by KF in (20), when the KF is initialized with $x_1 \sim \mathcal{N}(0, \Sigma)$. Notice that the true KF would use all past information, including $u_{-\infty:0}, y_{-\infty:0}$ to infer the true posterior distribution of x_1 . On the other hand, due to the finite length of the trajectories in the trajectory library, our CGM can only leverage information collected starting from time 1, which creates a mismatch between our CGM and the true KF. However, we shall show in the next subsection, that this discrepancy decays exponentially with respect to T_{ini} and hence is negligible in practice.

B. Optimality Gap with KF

In this subsection, we quantify the discrepancy between the asymptotic distribution of \bar{y}_f and the distribution predicted by the correctly initialized KF.

We begin by deriving the posterior distribution of y_f from the true KF. Recall from Section II that the behavioral model relies solely on the most recent T_{ini} I/O samples, while the trajectory may extend beyond this finite window. In contrast, we assume that the KF has access to the entire historical trajectory, $u_{-\infty:T_{ini}}, y_{-\infty:T_{ini}}$, along with the initial state distribution $\mathcal{N}(\mu_T, \Sigma_T)$. Given the linear system (1) and the initial state, the KF recursion is [38]:

$$\begin{aligned}\hat{x}_t &= \hat{x}_t^- + K_t(y_t - C\hat{x}_t^-), \quad P_t = (I - K_t C)P_t^-, \\ \hat{x}_{t+1} &= A\hat{x}_t + Bu_t, \quad P_{t+1} = AP_t A^\top + Q,\end{aligned}\quad (25)$$

with $K_t = P_t^- C^\top (CP_t^- C^\top + R)^{-1}$.

Proposition 5 (Predicted Distribution of KF). *Under Assumption 3-1), consider the KF (25) initialized with*

(μ_T, Σ_T) and updated recursively using the past samples $u_{-\infty:0}, y_{-\infty:0}$. Let \hat{x}_1^- and P_1^- denote the estimate of (25) at time $t = 1$. Conditioned on $(\mathcal{F}_{T_{ini}}, u_f)$, the distribution of y_f generated by the system (1) is Gaussian with mean

$$\hat{y}_f^* = \eta_f(P_1^-)z_{T_{ini}} + O_f \hat{\psi}_{T_{ini}+1}(P_1^-) \hat{x}_1^-,$$

and covariance

$$\mathcal{Y}_f^* = O_f P_{T_{ini}+1}^-(P_1^-) O_f^\top + G_f Q_f G_f^\top + R_f. \quad (26)$$

Similar to Proposition 3, the forms in this proposition follow directly from the linear structure of the recursive equations of KF.

The distribution given by the KF in Proposition 5 can be interpreted in two phases:

- 1) From $t = -\infty$ to 0: Estimate the distribution (\hat{x}_1^-, P_1^-) of x_1 using the input-output samples $u_{-\infty:0}, y_{-\infty:0}$ and the initial state distribution (μ_T, Σ_T) ;
- 2) From $t = 1$ to T_{ini} : First estimate $x_{T_{ini}+1}$ using u_{ini}, y_{ini} as in (25), and then predict y_f using u_f and the estimated $x_{T_{ini}+1}$ as described in (20).

Notably, the predictions in (26) coincide with the asymptotic distribution of the CGM in Theorem 4, with the only difference being initializations on the distribution of x_1 : $(0, \Sigma)$ for the asymptotic distribution of the CGM and (\hat{x}_1^-, P_1^-) for the KF.

The following theorem establishes that the gap between the asymptotic distribution and the distribution given by the KF decreases exponentially as the length of the initial trajectory $T_{ini} \rightarrow \infty$. The proof of the theorem is provided in Appendix III.

Theorem 6 (Gap with the optimal generative model). *Under Assumptions 1–3, and suppose $(A, Q^{1/2})$ is stabilizable. Let Σ and P_1^- be any positive definite matrices. As the initial horizon length T_{ini} tends to infinity, the conditional mean and covariance of the generated samples \hat{y}_f converge exponentially to those of the optimal generative model described in Proposition 5. More precisely, there exists a constant $0 < \rho < 1$ such that*

$$\begin{aligned} \lim_{T_{ini} \rightarrow \infty} \|\eta_f(\Sigma) - \eta_f(P_1^-)\| \rho^{-T_{ini}} &= 0, \\ \lim_{T_{ini} \rightarrow \infty} \|O_f \hat{\psi}_{T_{ini}+1}(P_1^-)\| \rho^{-T_{ini}} &= 0 \\ \lim_{T_{ini} \rightarrow \infty} \|\mathcal{Y}_f(\Sigma) - \mathcal{Y}_f(P_1^-)\| \rho^{-T_{ini}} &= 0. \end{aligned} \quad (27)$$

V. EXTENSION TO SYSTEMS WITH NON-GAUSSIAN NOISE

The convergence analysis in Section IV is specifically developed for systems with Gaussian noise, where the Bayesian optimal predictor reduces to the closed-form KF that our CGM asymptotically recovers. For systems with non-Gaussian noise, the Bayesian optimal estimator becomes nonlinear and typically lacks closed-form expressions. Although nonlinear Bayesian estimators can in principle approximate such posteriors, commonly used methods such as particle filters often suffer from computational complexity, particle degeneracy, and the curse of dimensionality [39].

Consequently, linear filtering approaches remain widely adopted in practice for their robustness and efficiency, even in non-Gaussian settings. Motivated by this, we next establish the optimality of our CGM among all linear predictors for systems with non-Gaussian noise. We first introduce the following assumptions:

Assumption 4. 1) The random variables $\{w_t\}$ and $\{v_t\}$ form i.i.d. sequences with zero mean and finite second moments. Moreover, the joint distribution of (ϕ_1, v_0, v_0) has support with nonempty interior.

2) For the multi-trajectory behavior library $\check{\mathcal{D}}^{(N)}$, the initial state $\check{x}_1^{(i)}$ of each trajectory is independently sampled from the same distribution with zero mean and covariance $\check{\Sigma} \succ 0$. Moreover, we assume that $\check{\Sigma} - \check{\Sigma}_{x\phi} \Sigma_\phi^\dagger \check{\Sigma}_{x\phi}^\top \succ 0$, where $\check{\Sigma}_{x\phi} = \mathbb{E}(\check{x}_1^{(1)} \check{\phi}_1^{(1)\top})$ and Σ_ϕ is introduced in Assumption 2.

Remark 8. Assumption 4 ensures that $\Xi^{(N)}$ has full row rank almost surely and that the equality constraint in (16) in our algorithm is therefore feasible.

Notably, under Assumption 4, the KF serves as the optimal estimator among all linear estimators in the minimum mean square error sense, even for systems with non-Gaussian noise:

Proposition 7 ([40]). *Consider the system (1) under Assumption 4. Let the KF recursion (25) be initialized with (μ, Σ) and applied over (u_{ini}, y_{ini}, u_f) . Then, the KF produces the MMSE prediction of y_f among all linear estimators with mean*

$$\hat{y}_f = \eta_f(\Sigma) z_{T_{ini}} + O_f \hat{\psi}_{T_{ini}+1}(\Sigma) \mu,$$

and covariance

$$\hat{\mathcal{Y}}_f(\Sigma) = O_f P_{T_{ini}+1}^-(\Sigma) O_f^\top + G_f Q_f G_f^\top + R_f.$$

The definition of $\eta_f, \hat{\psi}_{T_{ini}+1}, P_{T_{ini}+1}^-, O_f, G_f, Q_f, R_f$ is the same as that in Proposition 3.

The following proposition extends our convergence results in Theorem 4 and Theorem 6 to systems with non-Gaussian noise:

Proposition 8 (Extension to systems with non-Gaussian noise). *Under Assumption 1–4, the following results hold:*

1) The coefficients of the conditional mean and covariance of samples generated by CGM converge almost surely to their linear-MMSE counterparts:

$$\lim_{N \rightarrow \infty} \frac{\|\Theta_f^{(N)} - \eta_f(\Sigma)\|}{N^{-0.5+\epsilon}} = 0 \text{ a.s.}, \quad (28)$$

$$\lim_{N \rightarrow \infty} \frac{\|\Sigma_f^{(N)} - \mathcal{Y}_f(\Sigma)\|}{N^{-0.5+\epsilon}} = 0 \text{ a.s.}, \quad (29)$$

where Σ shares the same expression as in Theorem 4.

2) The exponential convergence with respect to T_{ini} established in Theorem 6 remains valid in the non-Gaussian setting, with the same convergence rate.

The proof of the proposition is included in Appendix II. This result demonstrates that our framework achieves the

best possible linear estimation with correct mean/variance propagation asymptotically, even in non-Gaussian settings.

VI. DIRECT DATA-DRIVEN PREDICTIVE CONTROL VIA CONDITIONAL GENERATIVE MODELING

This section presents data-driven predictive control approaches based on the proposed CGM. We develop the control formulations for systems with Gaussian noise, which enables a clear and tractable analysis. First, we introduce a data-driven “pessimistic” controller inspired by the scenario-based stochastic MPC. Subsequently, we introduce an alternative interpretation of DeePC [9]. Building on this interpretation, we formulate an “optimistic” controller that incorporates the proposed CGM to effectively capture the stochastic characteristic of the system.

A. Predictive Controller Inspired by Scenario-based MPC

Scenario-based Stochastic MPC (SSMPC) [41] is a powerful framework for solving finite-horizon constrained control problems for stochastic systems when complete parametric models are available. Specifically, for the stochastic system (1) with Gaussian noise characterized by state-space parameters A, B, C and noise covariances Q, R , the SSMPC solves the following control problem [42] at time T_{ini} over horizon T by generating M noise scenarios:

Problem 1 (Scenario-based stochastic MPC).

$$\begin{aligned} & \min_{u_f, y_f^{(j)}, x_t^{(j)}} \sum_{j=1}^M J\left(y_f^{(j)}, u_f\right), \\ \text{s.t. } & x_{t+1}^{(j)} = Ax_t^{(j)} + But + w_t^{(j)}, y_t^{(j)} = Cx_t^{(j)} + v_t^{(j)}, \\ & x_{T_{ini}+1}^{(j)} = \bar{x}_{T_{ini}+1}^{-(j)}, \\ & y_t^{(j)} \in \mathcal{Y}, u_t \in \mathcal{U}, \\ & \forall t = T_{ini} + 1, \dots, T_{ini} + T, j = 1, \dots, M, \end{aligned} \quad (30)$$

where $u_f = \text{col}(u_{T_{ini}+1}, \dots, u_{T_{ini}+T}), y_f^{(j)} = \text{col}(y_{T_{ini}+1}^{(j)}, \dots, y_{T_{ini}+T}^{(j)})$, and J denotes the cost function of the control problem. $w_t^{(j)}, v_t^{(j)}$ and $\hat{x}_{T_{ini}+1}^{-(j)}$ are samples drawn from $\mathcal{N}(0, Q), \mathcal{N}(0, R)$ and $\mathcal{N}(\hat{x}_{T_{ini}+1}^{-(j)}, P_{T_{ini}+1})$ respectively, and are treated as fixed scenarios in (31). Here, $\hat{x}_{T_{ini}+1}^{-(j)}, P_{T_{ini}+1}$ are obtained from the corresponding Kalman filter of system (1). \mathcal{Y} and \mathcal{U} are the feasible sets of outputs and inputs, respectively.

Notice that SSMPC requires full access to the state-space parameters A, B, C and the noise covariance Q, R of the system (1). In contrast, we construct a *direct data-driven* predictive controller by replacing the model-based scenario generation in (31) with samples generated by our CGM. Specifically, given dataset $\mathcal{D}^{(N)}$ collected offline, and T_{ini} historical sample pairs u_{ini}, y_{ini} of the current trajectory, we formulate the following optimization problem:

Problem 2 (SSMPC inspired Direct Data-Driven Predictive Control).

$$\begin{aligned} & \min_{u_f, y_f^{(j)}, \alpha^{(j)}} \sum_{j=1}^M J\left(y_f^{(j)}, u_f\right), \\ \text{s.t. } & \alpha^{(j)} = (\arg \min_g \|g\|_2^2 \mid \Xi^{(N)} g = \text{col}(0, z_{T_{ini}})), \\ & + (\beta^{(j)} \mid \Xi^{(N)} \beta^{(j)} = 0), y_f^{(j)} = Y_f^{(N)} \alpha^{(j)}, \\ & z_{T_{ini}} = \text{col}(u_{ini}, y_{ini}, u_f), \\ & y_t^{(j)} \in \mathcal{Y}, u_t \in \mathcal{U}, \\ & t = T_{ini} + 1, \dots, T_{ini} + T, j = 1, \dots, M, \end{aligned} \quad (32)$$

where each $\beta^{(j)}$ is a sample from $\mathcal{N}(0, \frac{1}{N} I_N)$ and is treated as fixed in the optimization problem.

This problem is formulated in a behavioral manner, as it only involves the trajectory library $\mathcal{D}^{(N)}$ and the initial trajectory u_{ini}, y_{ini} . Similar to SSMPC, this formulation is convex and can be efficiently solved using standard optimization tools, as long as the control cost J is convex and \mathcal{U}, \mathcal{Y} are convex sets. However, in contrast to SSMPC methods, which require the application of a Kalman filter and an optimization problem, both of which depend on precise system parameters, our approach is purely behavioral, avoiding an additional step for explicit system identification.

B. Discussions: Relationship with DeePC

This subsection provides an alternative interpretation of DeePC [9] through the lens of the proposed CGM. DeePC is a recently developed direct data-driven control method that leverages the Willems’ lemma [20] to predict system behavior and formulate the following control problem:

Problem 3 (DeePC for noisy systems).

$$\begin{aligned} & \min_{u_f, y_f, g, \sigma_y, \sigma} J(y_f, u_f) + \gamma_g h_g(g) + \gamma_y h_y(\sigma_y), \\ \text{s.t. } & Z^{(N)} g = (z_{T_{ini}} + \sigma), \quad y_f = Y_f^{(N)} g, \end{aligned} \quad (33)$$

$$\begin{aligned} & \sigma = \text{col}(0, \sigma_y, 0), \quad z_{T_{ini}} = \text{col}(u_{ini}, y_{ini}, u_f), \\ & y_t \in \mathcal{Y}, u_t \in \mathcal{U}, \quad \forall t = T_{ini} + 1, \dots, T_{ini} + T, \end{aligned} \quad (34)$$

where γ_g, γ_y are weighting parameters h_g, h_y denote penalty functions on g and σ_y , respectively.

Remark 9. Various regularizers have been proposed in DeePC with different rationales: ℓ_1 -norms for distributional robustness [9], [10], ℓ_2 -norms for computational simplicity and ridge-type interpretation [21], and projection-based terms for consistency with system identification [16].

Notice that in this problem, (33) represents a behavior model for the noisy system (1), where g and σ_y are related to the noise contained in the trajectory library \mathcal{D} and the collected past outputs y_{ini} , respectively. Based on this model, Problem 3 seeks to jointly minimize two competing objectives: the control cost and the deviation of the optimization

variables y_f from the future outputs determined by $\mathcal{D}^{(N)}$ and the past data of the current trajectory.

Two observations regarding this formulation can be made: First, Problem 3 adopts an optimistic stance toward noise, as the noise is treated as an optimization variable to minimize the control objective, instead of conforming to its correct distribution (stochastic formulation) [41] or serving as an adversarial element against minimizing the control objective (robust formulation) [43]. Secondly, for the Gaussian system (1), the distribution of the predicted y_f by the model in (33) may not effectively characterize the distribution of y_f of the true system.

To alleviate the model-mismatch issue in the second observation, we replace the behavior model in Problem 3 with our CGM introduced in Section III. Following the same logic as in Problem 3, we treat the noise component β in our CGM as an optimization variable, rather than a random variable. Our objective function also jointly minimizes the control cost and the deviation of the optimization variable y_f from the future outputs predicted by the CGM. The latter goal is achieved by maximizing the log-likelihood $\mathcal{L}(y_f \mid z_{T_{ini}}; \mathcal{D}^{(N)})$ of observing the generated y_f given the initial trajectory $z_{T_{ini}}$. The resulting control problem is then formulated as:

$$\begin{aligned} & \min_{u_f, y_f, \alpha, \beta} J(u_f, y_f) - \gamma \mathcal{L}(y_f \mid z_{T_{ini}}; \mathcal{D}^{(N)}), \\ \text{s.t. } & \alpha = (\arg \min_g \|g\|_2^2 \mid \Xi^{(N)} g = \text{col}(0, z_{T_{ini}})) \\ & + (\beta \mid \Xi^{(N)} \beta = 0), \\ & y_f = Y_f^{(N)} \alpha, \quad z_{T_{ini}} = \text{col}(u_{ini}, y_{ini}, u_f), \\ & y_t \in \mathcal{Y}, u_t \in \mathcal{U}, \forall t = T_{ini} + 1, \dots, T_{ini} + T. \end{aligned} \quad (35)$$

Similar to Problem 3, the hyperparameter γ balances the control cost and the model consistency.

The following proposition derives an equivalent expression of \mathcal{L} for the Gaussian system (1):

Proposition 9. *The log-likelihood function $\mathcal{L}(y_f \mid z_{T_{ini}}; \mathcal{D}^{(N)})$ has the following explicit expansion:*

$$\begin{aligned} \mathcal{L}(y_f \mid z_{T_{ini}}; \mathcal{D}^{(N)}) = & -\frac{N}{2} \|Y_f^{(N)}(I - \Xi^{(N)\dagger}\Xi^{(N)})\beta\|_{\Gamma^{-1/2}}^2 \\ & - \frac{Tp}{2} \log(2\pi) - \frac{1}{2} \log \det(\frac{1}{N}\Gamma), \end{aligned} \quad (36)$$

where $\Gamma = Y_f^{(N)}(I - \Xi^{(N)\dagger}\Xi^{(N)})(I - \Xi^{(N)\dagger}\Xi^{(N)})^\top Y_f^{(N)\top}$ and $\|x\|_{\Gamma^{-1/2}} = \sqrt{x^\top \Gamma^{-1} x}$.

This proposition follows from the standard log-likelihood function for multivariate Gaussian distributions [44]. Using Proposition 9, we can derive another stochastic variant of DeePC in (33):

Problem 4 (Variant of DeePC based on our CGM).

$$\begin{aligned} & \min_{u_f, y_f, \alpha, \beta} J(y_f, u_f) + \tilde{\gamma} \|Y_f^{(N)}(I - \Xi^{(N)\dagger}\Xi^{(N)})\beta\|_{\Gamma^{-1/2}}^2, \\ \text{s.t. } & \alpha = (\arg \min_g \|g\|_2^2 \mid \Xi^{(N)} g = z_{T_{ini}}) \\ & + (\beta \mid \Xi^{(N)} \beta = 0), \\ & y_f = Y_f^{(N)} \alpha, \quad z_{T_{ini}} = \text{col}(u_{ini}, y_{ini}, u_f), \\ & y_t \in \mathcal{Y}, u_t \in \mathcal{U}, \quad \forall t = T_{ini} + 1, \dots, T_{ini} + T. \end{aligned} \quad (37)$$

Similar to Problem 3, maximizing the likelihood function also leads to a regularization term, which better aligns with the stochastic properties of the system.

Finally, we note that by setting the random part β in our CGM of Problem 4 to zero, the controller reduces to a data-driven deterministic controller. Moreover, if $\Phi^{(N)} = 0$ in addition to $\beta = 0$, the resulting controller coincides with the Subspace Predictive Controller (SPC) [45]. Hence, this establishes SPC as a data-driven version of the deterministic MPC, where only the expectation of the predicted outputs are considered. Simulation results in Section VII compares its performance with both deterministic MPC and DeePC.

VII. SIMULATIONS

This section presents simulations to assess the effectiveness of the proposed model. We focus on the trajectory tracking problem of a 4-dimensional single-input, single-output three-pulley system, originally introduced in [46] and subsequently studied in [16], [19], [47], [48]. The system parameters are consistent with those in [48]. Both process and observation noise are modeled as Gaussian with zero mean and covariances of $Q = 0.01I$ and $R = 0.04I$, respectively.

A. Convergence Speed Verification

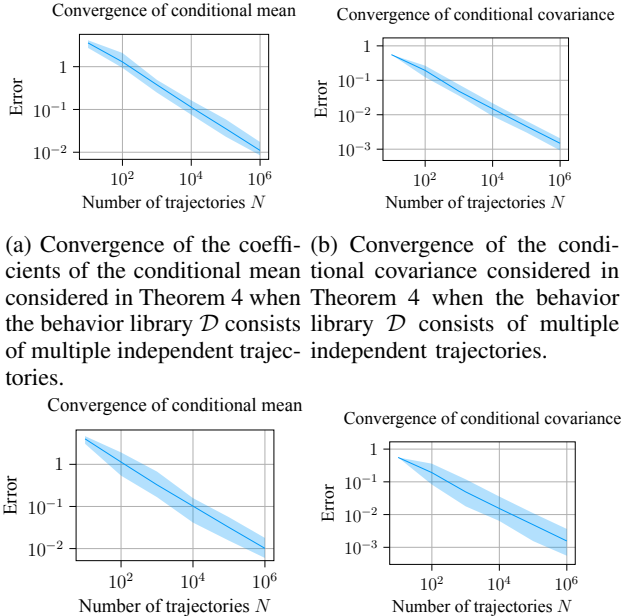
We perform experiments to evaluate the convergence speed in Theorem 4. For the CGM, we set the length of initial trajectory to $T_{ini} = 8$ and the prediction horizon to $T = 10$. Each experiment is repeated independently for 100 times, and the results are presented in Fig. 1. The figures show that the convergence speed is approximately $O(N^{-0.5})$ in both cases, supporting the validity of Theorem 4.

B. Control Performance Comparison

We next compare the control performance of the direct data-driven predictive controllers proposed in Section VI.

Controller Implementations: We implement three groups of controllers:

- **Deterministic controllers:** We implement several deterministic control approaches for comparison. First, we reproduce a classic model-based controller combining Kalman filtering with deterministic MPC (KF+DMPC), where the state-space parameters are set to the true system parameters. We also implement the Subspace Predictive Controller (SPC) [45], which can be viewed as a deterministic variant of our proposed optimistic controller in Problem 4. Additionally, we include a traditional data-driven control approach that first identifies



(a) Convergence of the coefficients of the conditional mean considered in Theorem 4 when the behavior library \mathcal{D} consists of multiple independent trajectories.

(b) Convergence of the conditional covariance considered in Theorem 4 when the behavior library \mathcal{D} consists of multiple independent trajectories.

(c) Convergence of coefficients of the conditional mean considered in Theorem 4 when the behavior library \mathcal{D} is a single trajectory.

(d) Convergence of the conditional covariance considered in Theorem 4 when the behavior library \mathcal{D} is a single trajectory.

Fig. 1: Convergence speed verification of the proposed generative model as the number of trajectories N (or equivalently, the length of the single trajectory) increases. The figures depict a log-log ribbon plot, with the solid line indicating the mean value and the shaded region representing the range of values.

state-space parameters using the Ho-Kalman algorithm, then applies Kalman filtering and deterministic MPC (Ho-Kalman+KF+DMPC) [49].

- **“Optimistic” controllers:** We implement DeePC, as described in Problem 3, γ -DDPC [50] and our variant of DeePC from Problem 4 with $\tilde{\gamma} = 1000$. To enhance computational efficiency and improve the performance of DeePC, following [16], [21], we specify the regularization term in Problem 3 as:

$$\gamma_y \|\sigma_y\|_2^2 + \gamma_Z \|(I - Z^{(N)\dagger} Z^{(N)})g\|_2^2,$$

where we set $\gamma_y = 100$ and $\gamma_Z = 10^6$.

- **Scenario-based stochastic controllers:** We implement a classic model-based controller, specifically a KF combined with an SSMPMC (KF+SSMPMC), as described in Problem 1, where the state-space parameters and noise covariances are set to the true system parameters. We also implement an oracle controller (Oracle SSMPMC with perfect x_t) that assumes perfect knowledge of both system parameters and current states x_t at each time step. Additionally, we construct our proposed scenario-based predictive controller equipped with our generative model, as described in Problem 2, for comparison. This controller is denoted as Scenario-based Stochastic PC with generative model (SSPC_{gen}). In all controllers, we use $M = 50$ scenarios to account for system

uncertainty.

Experimental Setup: All experiments start from the zero initial state. Following [51], the controllers apply zero inputs for the first $T_{ini} = 8$ time steps to collect the initial trajectory (u_{ini}, y_{ini}) . After this initialization period, each controller operates in closed loop for 100 time steps. The control objective is similar to [9], defined as:

$$J(y_f, u_f) = \sum_{t=T_{ini}+1}^{T_{ini}+T} (\|y_t - 10\|_2^2 + 0.01\|u_t\|_2^2). \quad (38)$$

The constraints are $y_t \leq 12, t = T_{ini} + 1, \dots, T_{ini} + T$. The horizon for all controllers is set to $T = 10$. For the data-driven controllers, we generate single long trajectories with i.i.d. Gaussian inputs, with trajectory lengths $K = 117$ and $K = 1017$, setting $T_{ini} = 8$ and $T = 10$. These trajectory lengths allow us to construct Hankel matrices with $N = 100$ and $N = 1000$ columns respectively, following the relationship $N = K - T_{ini} - T + 1$, to formulate the trajectory library $\mathcal{D}^{(N)}$. We perform 100 independent experiments, reporting the average control cost across experiments with no constraint violations, along with the probability of constraint violation, defined as

$$p_{fail} = \frac{N_{fail}}{N_{trial}},$$

where N_{fail} denotes the number of experiments with constraint violations, and N_{trial} denotes the total number of experiments. Constraint violations are monitored and recorded throughout the entire closed-loop operation. The results are presented in Table I.

Simulation results show that while KF+DMPC achieves a competitive average control cost of 436.94, it incurs a relatively high constraint violation probability of 0.19. When the size of the trajectory library is rather limited ($N = 100$), SPC and Ho-Kalman+KF+DMPC have violation probabilities of 0.20 and 0.56, respectively. The particularly poor performance of Ho-Kalman+KF+DMPC with $N = 100$ (average cost of 1087.97 and violation probability of 0.56) can be attributed to the sensitivity of the Ho-Kalman algorithm to noise in limited data [52], [53], leading to inaccurate identification of system parameters A, B, C and consequently poor control performance. However, both algorithms demonstrate significant improvement as the trajectory library size N increases, with SPC reducing its control cost to 438.25 and Ho-Kalman+KF+DMPC achieving substantial improvements in both cost (466.99) and violation probability (0.23) at $N = 1000$. Additionally, DeePC, γ -DDPC and our $\text{DeePC}_{var, \tilde{\gamma}}$ exhibit suboptimal performance in terms of constraint satisfaction, although increasing the trajectory library size N enhances their reliability. These results show that an optimistic approach to noise in controller design can compromise robustness.

In contrast, KF+SSMPMC reduces the violation probability to 0.00, while maintaining a competitive control cost of 439.88, demonstrating the importance of incorporating stochastic models for ensuring constraint satisfaction, particularly in safety-critical applications. Additionally, our

Controller	Average Cost	p_{fail}	Online computation time per step (ms)
KF+Deterministic MPC (KF+DMPC)	436.94	0.19	2.30
SPC ($N = 100$)	443.12	0.20	2.62
SPC ($N = 1000$)	438.25	0.20	2.58
Ho-Kalman+KF+Deterministic MPC (Ho-Kalman+KF+DMPC, $N = 100$)	1087.97	0.56	2.30
Ho-Kalman+KF+Deterministic MPC (Ho-Kalman+KF+DMPC, $N = 1000$)	466.99	0.23	2.30
DeePC ($N = 100$)	450.60	0.18	7.62
DeePC ($N = 1000$)	438.50	0.14	792.07
γ -DDPC ($N = 100$)	443.02	0.19	1.13
γ -DDPC ($N = 1000$)	438.25	0.20	1.92
Our variant of DeePC ($N = 100, \tilde{\gamma} = 1000$, $\text{DeePC}_{var, \tilde{\gamma}}$)	443.06	0.20	10.43
Our variant of DeePC ($N = 1000, \tilde{\gamma} = 1000$, $\text{DeePC}_{var, \tilde{\gamma}}$)	438.41	0.14	865.17
Oracle SSMPMC with perfect xt	432.26	0.01	9.69
KF+SSMPMC (KF+SSMPMC)	439.88	0.00	10.99
Scenario-based stochastic PC with CGM ($N = 100$, SSPC_{gen})	440.73	0.05	13.33
Scenario-based stochastic PC with CGM ($N = 1000$, SSPC_{gen})	437.32	0.01	12.67

TABLE I: Average control cost, constraint violation probability p_{fail} and online computation times for the deterministic controllers, “optimistic” controllers and scenario-based stochastic controllers, respectively, over 100 independent experiments.

proposed SSPC_{gen} outperforms both the deterministic and optimistic controllers, achieving violation probabilities of 0.05 and 0.01 for $N = 100$ and $N = 1000$ respectively, while maintaining control costs of 440.73 and 437.32. As the size of the trajectory library N increases, SSPC_{gen} approaches the performance of SSMPMC, which relies on true system parameters. This result further validates the effectiveness of the proposed generative model in accounting for system uncertainties and enhancing the robustness of predictive controllers against system noise.

Table I also compares the online computation time per step for all controllers. The “optimistic” approaches (DeePC and $\text{DeePC}_{var, \tilde{\gamma}}$) require significantly longer computation times, especially with large trajectory libraries, with computation times increasing from 7.62ms to 792.07ms for DeePC and from 10.43ms to 865.17ms for $\text{DeePC}_{var, \tilde{\gamma}}$ as N increases from 100 to 1000. In contrast, our SSPC_{gen} and SPC, which are data-driven counterparts of SSMPMC and KF+DMPC respectively, achieve comparable computational efficiency to their model-based versions, with SSPC_{gen} and SPC requiring only 13.33ms and 2.62ms for $N = 100$ respectively. Moreover, their computation times remain stable with increasing library size, demonstrating their strong scalability.

At online deployment, we apply the proposed scenario-based stochastic predictive controller with the CGM (SSPC_{gen}) on an unstable system. The objective, constraint set, and horizons are the same as in the preceding simulations; only the state-space matrices (A, B, C) differ as follows:

$$A = \begin{bmatrix} 1.10 & 0.20 \\ 0.00 & 0.98 \end{bmatrix}, \quad B = \begin{bmatrix} 0.50 \\ 0.20 \end{bmatrix}, \quad C = \begin{bmatrix} 1.00 & 0.00 \end{bmatrix}.$$

We also use $M = 50$ scenarios per step. Performance metrics are kept the same as the preceding subsection, and the experimental results are reported in Table II.

The simulation results demonstrate that the proposed CGM-based SSPC can effectively handle open-loop unstable systems. With data collected under the pre-stabilized output-feedback excitation, the controller achieves stable and constraint-satisfying performance, maintaining tracking accuracy comparable to the stable-plant case. These results confirm that the proposed method seamlessly extends to un-

stable dynamics while preserving strong control performance and robustness.

VIII. CONCLUSION

This paper proposes a behavioral CGM for stochastic LTI systems. The model generates random samples from the data-driven approximation of the conditional distribution of future outputs given past inputs and outputs, ensuring consistency with the system’s trajectory library. It is purely behavioral, utilizing only the I/O samples of the system without explicit system identification. We analyze the model’s performance by proving that the distribution of generated samples converges as the size of the trajectory library increases. Additionally, we prove that the gap between the asymptotic distribution as N tends to infinity and the distribution of the optimal CGM decays exponentially with the length T_{ini} of the initial trajectory. The proposed model is then incorporated into a predictive control framework, formulating a direct data-driven predictive control problem that accounts for the system’s stochastic characteristics while bypassing the identification steps and state estimations. Numerical results validate the derived bounds and demonstrate the model’s effectiveness in enhancing the robustness of predictive controllers under system noise.

APPENDIX I PROOF OF PROPOSITION 3

Proof. Consider the current recorded initial trajectory $z_{T_{ini}}$ beginning at $t = 1$ and evolving to the current time step T_{ini} . The KF recursively computes state estimates according to (25), initialized with $\hat{x}_1^- = \mu$ and $P_1^- = P$. Then, the optimal estimation for $x_{T_{ini}+1}^-$ conditioned on u_{ini}, y_{ini} is $\hat{x}_{T_{ini}+1}^-$ with covariance $P_{T_{ini}+1}^-$.

From the Kalman filter recursion (25), we observe that $\hat{x}_{T_{ini}+1}^-$ depends linearly on the measurements y_{ini} , inputs u_{ini} , and the initial mean μ . By the linearity of the Kalman filter, this relationship can be expressed as:

$$\hat{x}_{T_{ini}+1}^- = \hat{\theta}_{T_{ini}+1}^-(P) \text{col}(u_{ini}, y_{ini}) + \hat{\psi}_{T_{ini}+1}^-(P)\mu, \quad (39)$$

where $\hat{\theta}_{T_{ini}+1}^- : \mathbb{R}^{n \times n} \rightarrow \mathbb{R}^{n \times (T_{ini}(m+p))}$ and $\hat{\psi}_{T_{ini}+1}^- : \mathbb{R}^{n \times n} \rightarrow \mathbb{R}^n$ are functions of the initial state covariance P , whose explicit forms can be computed recursively from (25)

Controller	Average Cost	p_{fail}	Online computation time per step (ms)
Scenario-based stochastic PC with CGM ($N = 100$, SSPC_{gen})	122.16	0.00	11.87
Scenario-based stochastic PC with CGM ($N = 1000$, SSPC_{gen})	118.69	0.00	12.21

TABLE II: Average control cost, constraint violation probability p_{fail} and online computation times for scenario-based stochastic controllers, over 100 independent experiments for an open-loop unstable system.

but are omitted for brevity. The expressions also depend on the state-space parameters A, B, C, Q, R , which are omitted in the notation for simplicity. We similarly treat $P_{T_{ini}+1}^- : \mathbb{R}^{n \times n} \rightarrow \mathbb{R}^{n \times n}$ as a function of P , denoted as $P_{T_{ini}+1}^-(P)$.

Then, based on the estimated distribution of the state $x_{T_{ini}+1}$, we can provide multi-step ahead predictions for future outputs y_f . Define $w_f = \text{col}(w_{T_{ini}+1}, \dots, w_{T_{ini}+T})$, $v_f = \text{col}(v_{T_{ini}+1}, \dots, v_{T_{ini}+T})$ and

$$O_f = [C^\top \quad (CA)^\top \quad \dots \quad (CA^{T-1})^\top]^\top,$$

$$G_f = \begin{bmatrix} 0 & 0 & \dots & 0 & 0 \\ C & 0 & \dots & 0 & 0 \\ \vdots & \vdots & \ddots & \vdots & \vdots \\ CA^{T-3} & CA^{T-4} & \dots & 0 & 0 \\ CA^{T-2} & CA^{T-3} & \dots & C & 0 \end{bmatrix},$$

$$H_f = G_f(I_T \otimes B), Q_f = (I_T \otimes Q), R_f = (I_T \otimes R).$$

By unrolling the system dynamics (1) over the prediction horizon T , the relationship between future outputs y_f , the state $x_{T_{ini}+1}$ and future inputs u_f is given by:

$$y_f = O_f x_{T_{ini}+1} + H_f u_f + G_f w_f + v_f.$$

Using this relationship, the mean of y_f conditioned on u_{ini}, y_{ini}, u_f is:

$$\begin{aligned} \mathbb{E}(y_f | z_{T_{ini}}) &= O_f \hat{x}_{T_{ini}+1}^- + H_f u_f \\ &= \underbrace{[O_f \hat{\theta}_{T_{ini}+1}^-(P) \quad H_f]}_{\eta_f(P)} z_{T_{ini}} + O_f \hat{\psi}_{T_{ini}+1}^-(P) \mu, \end{aligned}$$

Since w_f, v_f are independent of $z_{T_{ini}}$, the conditional covariance is:

$$\begin{aligned} \mathcal{Y}_f(P) &\triangleq \text{Cov}(y_f | z_{T_{ini}}) \\ &= O_f P_{T_{ini}+1}^-(P) O_f^\top + G_f Q_f G_f^\top + R_f. \end{aligned} \quad \square$$

APPENDIX II

PROOFS OF THEOREM 4 AND COROLLARY 8

Both the conditional mean and covariance of \bar{y}_f depend fundamentally on the matrix

$$\begin{aligned} \mathcal{W}^{(N)} &= \frac{1}{N} \left[\Phi^{(N)\top} \quad Z^{(N)\top} \quad Y_f^{(N)\top} \right]^\top \left[\Phi^{(N)\top} \quad Z^{(N)\top} \quad Y_f^{(N)\top} \right]. \end{aligned}$$

For convenience of notation, when $\Phi^{(N)}, Z^{(N)}, Y_f^{(N)}$ carry tilde ($\tilde{\cdot}$) or check ($\check{\cdot}$), these modifiers extend to $\mathcal{W}^{(N)}$ correspondingly. Based on this definition, we first analyze the convergence property of $\mathcal{W}^{(N)}$ as N tends to infinity, which subsequently leads to the convergence of the conditional mean and covariance in Theorem 4.

A. Convergence of $\mathcal{W}^{(N)}$

To derive the asymptotic distribution of $\mathcal{W}^{(N)}$ for both behavior libraries $\tilde{\mathcal{D}}^{(N)}$ and $\check{\mathcal{D}}^{(N)}$, we first introduce several additional notations. For the multi-trajectory library $\check{\mathcal{D}}^{(N)}$ under Assumption 3, the corresponding random vectors $\{\check{u}_t^{(i)}, \check{y}_t^{(i)}, \check{\phi}_t^{(i)}\}_{t=1}^{T_{ini}+T}$ of the sampled trajectories are i.i.d. across different indices i . To formalize this statistical structure, we define a set of representative random vectors $\{\check{u}_t, \check{y}_t, \check{\phi}_t\}_{t=1}^{T_{ini}+T}$ that preserve the identical joint distribution shared by each trajectory $\{\check{u}_t^{(i)}, \check{y}_t^{(i)}, \check{\phi}_t^{(i)}\}_{t=1}^{T_{ini}+T}$. Define the composite random vector

$$\check{\vartheta}_t \triangleq \text{col}(\check{\phi}_1, \check{u}_{1:T_{ini}}, \check{y}_{1:T_{ini}}, \check{u}_{T_{ini}+1:T_{ini}+T}, \check{y}_{T_{ini}+1:T_{ini}+T}),$$

with the corresponding covariance matrix:

$$\check{\mathcal{W}} = \mathbb{E}(\check{\vartheta}_t \check{\vartheta}_t^\top).$$

On the other hand, for the single-trajectory library $\tilde{\mathcal{D}}^{(N)}$, let $\tilde{y}_{t,f}$ and $\tilde{z}_{t,T_{ini}}$ denote the random vectors corresponding to the t -th column of $\tilde{Y}_f^{(N)}$ and $\tilde{Z}^{(N)}$, respectively:

$$\tilde{y}_{t,f} = \text{col}(\tilde{y}_{t+T_{ini}}, \dots, \tilde{y}_{t+T_{ini}+T-1}),$$

$$\tilde{z}_{t,T_{ini}} = \text{col}(\tilde{u}_{t:t+T_{ini}-1}, \tilde{y}_{t:t+T_{ini}-1}, \tilde{u}_{t+T_{ini}:t+T_{ini}+T-1}).$$

Then, define the augmented vector

$$\tilde{\vartheta}_t \triangleq \left[\tilde{\phi}_t^\top \quad \tilde{z}_{t,T_{ini}}^\top \quad \tilde{y}_{t,f}^\top \right]^\top$$

and the corresponding asymptotic covariance matrix

$$\tilde{\mathcal{W}} = \bar{\mathbb{E}}_t(\tilde{\vartheta}_t \tilde{\vartheta}_t^\top) = \lim_{t \rightarrow \infty} \mathbb{E}(\tilde{\vartheta}_t \tilde{\vartheta}_t^\top). \quad (40)$$

We hereafter unify the notation of $\check{\mathcal{W}}$ and $\tilde{\mathcal{W}}$ as \mathcal{W} for simplicity.

For simplicity of notation, we introduce the following convergence rate notation. For a sequence of random variables, vectors, or matrices $\{x_t\}_{t \geq 1}$, we write $x_t \sim \mathcal{C}(\beta)$ if for all $\epsilon > 0$,

$$\lim_{t \rightarrow \infty} \frac{\|x_t\|}{t^{\beta+\epsilon}} = 0 \quad \text{almost surely},$$

where both $\|x_t\|/t^{\beta+\epsilon}$ and 0 are random variables. This notation indicates that x_t converges to zero at a rate faster than any polynomial of order β . Note that $\mathcal{C}(\beta)$ denotes a class of stochastic processes with a certain convergence rate, not a probability distribution.

We first recall the following result from [54], which establishes convergence rates for sample covariances of temporally correlated data from stable linear systems.

Lemma 10 ([54], Lemma 7). *Consider the autonomous LTI system (1) with $B = 0$ and stable matrix A (i.e., all*

eigenvalues of A lie strictly inside the unit circle). Then the sample covariance converges as

$$\frac{1}{k} \sum_{t=1}^k y_t y_t^\top - \bar{\mathbb{E}}_t(y_t y_t^\top) \sim \mathcal{C}(-0.5).$$

Then, we introduce the following result:

Lemma 11. Given the trajectory library $\mathcal{D}^{(N)}$, we have that:

$$\mathcal{W}^{(N)} - \mathcal{W} \sim \mathcal{C}(-0.5).$$

Proof. For the multi-trajectory library $\tilde{\mathcal{D}}^{(N)}$, the convergence of $\mathcal{W}^{(N)}$ to \mathcal{W} follows directly from the strong law of large numbers and the law of iterated logarithm.

For the single-trajectory library $\tilde{\mathcal{D}}^{(N)}$, we analyze $\tilde{\mathcal{W}}^{(N)}$ (the sample average of $\tilde{\vartheta}_t \tilde{\vartheta}_t^\top$) by constructing an augmented system with output $\tilde{\vartheta}_t$. Define the $T_{ini} + T$ -length windowed vector:

$$\tilde{\phi}_{t,T_{ini}:T} = \text{col}(\tilde{\phi}_t, \dots, \tilde{\phi}_{t+T_{ini}+T-1}),$$

$$\tilde{u}_{t,T_{ini}:T} = \text{col}(\tilde{u}_t, \dots, \tilde{u}_{t+T_{ini}+T-1}),$$

and $\tilde{y}_{t,T_{ini}:T}$ is similarly defined. Then, the augmented state vector becomes:

$$\tilde{\varphi}_t = \text{col}(\tilde{\phi}_{t,T_{ini}:T}, \tilde{u}_{t,T_{ini}:T}, \tilde{x}_{t+T_{ini}+T-1}, \tilde{y}_{t,T_{ini}:T}). \quad (41)$$

Define an augmented system with the following dynamics:

$$\tilde{\varphi}_{t+1} = \tilde{A}_\varphi \tilde{\varphi}_t + \tilde{w}_{\varphi,t}, \quad \tilde{\vartheta}_t = \text{col}(\tilde{\phi}_t, \tilde{z}_{t,T_{ini}}, \tilde{y}_{t,f}) = \tilde{C}_\varphi \tilde{\varphi}_t, \quad (42)$$

where \tilde{A}_φ can be derived based on the dynamics of the system and the controller, and is omitted here due to the space limit. The noise $\tilde{w}_{\varphi,t}$ is a structured vector containing zero entries and noise terms $w_{t+T_{ini}+T-1}, w_{t+T_{ini}+T-1}$ and their linear transformations, and \tilde{C}_φ is a selection matrix taking the corresponding elements from $\tilde{\varphi}_t$.

To prove the convergence of $\tilde{\mathcal{W}}^{(N)}$, we note that the primary challenge arises from the fact that the outputs $\tilde{\vartheta}_t$ of this augmented system are correlated across time, violating standard i.i.d. assumptions required for classical convergence results. However, since the augmented system in (42) is stable and driven by i.i.d. noise $\tilde{w}_{\varphi,t}$, it satisfies the conditions of Lemma 10. Therefore, by Lemma 10, the sample covariance of the temporally correlated outputs $\tilde{\vartheta}_t$ still converges at the standard rate, and it follows that:

$$\tilde{\mathcal{W}}^{(N)} - \tilde{\mathcal{W}} \sim \mathcal{C}(-0.5). \quad \square$$

B. Convergence of mean and covariance

Next, we are ready to consider the convergence of mean and covariance of \bar{y}_f . For convenience of expressing the asymptotic distribution, for the single-trajectory behavior library $\tilde{\mathcal{D}}^{(N)}$, let

$$\tilde{z}_{t,T_{ini}}^\perp = \tilde{z}_{t,T_{ini}} - \bar{\mathbb{E}}_t(\tilde{z}_{t,T_{ini}} \tilde{\phi}_t^\top) \bar{\mathbb{E}}_t(\tilde{\phi}_t \tilde{\phi}_t^\top)^\dagger \tilde{\phi}_t,$$

$$\tilde{y}_{t,f}^\perp = \tilde{y}_{t,f} - \bar{\mathbb{E}}_t(\tilde{y}_{t,f} \tilde{\phi}_t^\top) \bar{\mathbb{E}}_t(\tilde{\phi}_t \tilde{\phi}_t^\top)^\dagger \tilde{\phi}_t.$$

On the other hand, for the multi-trajectory library $\tilde{\mathcal{D}}^{(N)}$, define

$$\begin{aligned} \check{z}_{T_{ini}}^\perp &= \check{z}_{T_{ini}} - \mathbb{E}(\check{z}_{T_{ini}} \check{\phi}_1^\top) \mathbb{E}(\check{\phi}_1 \check{\phi}_1^\top)^\dagger \check{\phi}_1, \\ \check{y}_f^\perp &= \check{y}_f - \mathbb{E}(\check{y}_f \check{\phi}_1^\top) \mathbb{E}(\check{\phi}_1 \check{\phi}_1^\top)^\dagger \check{\phi}_1. \end{aligned}$$

Using these notations, we have the following convergence result:

Lemma 12. The coefficients in the mean of \bar{y}_f satisfies

$$\check{\Theta}_f^{(N)} - \check{\eta}_{f,\infty} \sim \mathcal{C}(-0.5), \quad \check{\Theta}_f^{(N)} - \check{\eta}_{f,\infty} \sim \mathcal{C}(-0.5),$$

where

$$\begin{aligned} \check{\eta}_{f,\infty} &= \bar{\mathbb{E}}_t(\tilde{y}_{t,f}^\perp \tilde{z}_{t,T_{ini}}^\perp) [\bar{\mathbb{E}}_t(\tilde{z}_{t,T_{ini}}^\perp \tilde{z}_{t,T_{ini}}^\perp)]^{-1}. \\ \check{\eta}_{f,\infty} &= \mathbb{E}(\check{y}_f^\perp \check{z}_{T_{ini}}^\perp) [\mathbb{E}_t(\check{z}_{T_{ini}}^\perp \check{z}_{T_{ini}}^\perp)]^{-1}. \end{aligned}$$

On the other hand, the covariance of the generated sample \bar{y}_f satisfies:

$$\check{\Sigma}_f^{(N)} - \check{\mathcal{Y}}_{f,\infty} \sim \mathcal{C}(-0.5), \quad \check{\Sigma}_f^{(N)} - \check{\mathcal{Y}}_{f,\infty} \sim \mathcal{C}(-0.5),$$

where

$$\begin{aligned} \check{\mathcal{Y}}_{f,\infty} &= \bar{\mathbb{E}}_t(\tilde{y}_{t,f}^\perp \tilde{y}_{t,f}^\perp) \\ &\quad - \bar{\mathbb{E}}_t(\tilde{y}_{t,f}^\perp \tilde{z}_{t,T_{ini}}^\perp) \bar{\mathbb{E}}_t(\tilde{z}_{t,T_{ini}}^\perp \tilde{z}_{t,T_{ini}}^\perp)^{-1} \bar{\mathbb{E}}_t(\tilde{z}_{t,T_{ini}}^\perp \tilde{y}_{t,f}^\perp), \\ \check{\mathcal{Y}}_{f,\infty} &= \mathbb{E}(\check{y}_f^\perp \check{y}_f^\perp) \\ &\quad - \mathbb{E}(\check{y}_f^\perp \check{z}_{T_{ini}}^\perp) \mathbb{E}(\check{z}_{T_{ini}}^\perp \check{z}_{T_{ini}}^\perp)^{-1} \mathbb{E}(\check{z}_{T_{ini}}^\perp \check{y}_f^\perp). \end{aligned} \quad (43)$$

Proof. This proof applies to both behavior libraries, so we omit the tilde and check accents. The key idea is to express the mean $\Theta_f^{(N)}$ and covariance $\Sigma_f^{(N)}$ as functions of $\mathcal{W}^{(N)}$, then establish their convergence using Lemma 3.3 from [54].

First, we derive the expression for $\Theta_f^{(N)}$. Recall that $\Theta_f^{(N)} z_{T_{ini}}$ represents the special solution:

$$Y_f^{(N)} (\arg \min_g \|g\|_2^2 \mid \text{col}(\Phi^{(N)}, Z^{(N)}) g = \text{col}(0, z_{T_{ini}})). \quad (44)$$

The constraint $\Phi^{(N)} g = 0$ implies $g = (I - \Phi^{(N)\dagger} \Phi^{(N)}) h$ for any $h \in \mathbb{R}^N$. Substituting this into the optimization problem in (44), we obtain the equivalent formulation:

$$\begin{aligned} &(\arg \min_h \| (I - \Phi^{(N)\dagger} \Phi^{(N)}) h \|_2^2 \mid \\ &Z^{(N)} (I - \Phi^{(N)\dagger} \Phi^{(N)}) h = z_{T_{ini}}). \end{aligned} \quad (45)$$

Let $Z^{(N)\perp} = Z^{(N)} (I - \Phi^{(N)\dagger} \Phi^{(N)})$. The equality constraint in (45) implies:

$$h = Z^{(N)\perp\dagger} z_{T_{ini}} + (I - Z^{(N)\perp\dagger} Z^{(N)\perp}) \tilde{h} \quad (46)$$

for any $\tilde{h} \in \mathbb{R}^N$. Then, the objective function becomes:

$$\begin{aligned} \|g\|_2^2 &= \| (I - \Phi^{(N)\dagger} \Phi^{(N)}) h \|_2^2 \\ &= \| (I - \Phi^{(N)\dagger} \Phi^{(N)}) Z^{(N)\perp\dagger} z_{T_{ini}} \|_2^2 \\ &\quad + \| (I - \Phi^{(N)\dagger} \Phi^{(N)}) (I - Z^{(N)\perp\dagger} Z^{(N)\perp}) \tilde{h} \|_2^2. \end{aligned}$$

The minimum is achieved at $\tilde{h} = 0$, yielding:

$$\begin{aligned} (\arg \min_g \|g\|_2^2 \mid \Xi^{(N)} g = \text{col}(0, z_{T_{ini}})) \\ = (I - \Phi^{(N)\dagger} \Phi^{(N)}) Z^{(N)\perp\dagger} z_{T_{ini}}. \end{aligned}$$

Define $Y_f^{(N)\perp} = Y_f^{(N)} (I - \Phi^{(N)\dagger} \Phi^{(N)})$. This leads to the simplified expression:

$$\Theta_f^{(N)} = Y_f^{(N)\perp} Z^{(N)\perp\dagger}.$$

Next, we establish the connection between $\mathcal{W}^{(N)}$ and $Y_f^{(N)\perp} Z^{(N)\perp\dagger}$. We prove in Appendix IV that $Z^{(N)\perp}$ has full row rank, which implies that:

$$\begin{aligned} Z^{(N)\perp\dagger} &= Z^{(N)\perp\top} (Z^{(N)\perp} Z^{(N)\perp\top})^{-1}, \\ Z^{(N)\perp} Z^{(N)\perp\top} &= Z^{(N)} Z^{(N)\top} - Z^{(N)} \Phi^{(N)\dagger} \Phi^{(N)} Z^{(N)\top}, \\ &= Z^{(N)} Z^{(N)\top} - Z^{(N)} \Phi^{(N)\top} (\Phi^{(N)} \Phi^{(N)\top})^\dagger \Phi^{(N)} Z^{(N)\top}, \end{aligned}$$

where the last equality can be verified by computing the pseudo-inverse of $\Phi^{(N)}$ using its singular value decomposition.

Then, we aim to express $Y_f^{(N)\perp} Z^{(N)\perp\dagger}$ as a differentiable function of $\mathcal{W}^{(N)}$. Consider a matrix $X \in \mathbb{R}^{(n_u + (T_{ini} + T)(p+m)) \times (n_u + (T_{ini} + T)(p+m))}$ with the same dimension as \mathcal{W} . For simplicity, we split X as follows:

$$X = \begin{bmatrix} X_{\phi\phi} & X_{\phi z} & X_{\phi y} \\ X_{z\phi} & X_{zz} & X_{zy} \\ X_{y\phi} & X_{yz} & X_{yy} \end{bmatrix}, \quad (47)$$

where $X_{\phi\phi} \in \mathbb{R}^{n_u \times n_u}$, $X_{yy} \in \mathbb{R}^{Tp \times Tp}$, $X_{zz} \in \mathbb{R}^{(T_{ini}(m+p) + Tm) \times (T_{ini}(m+p) + Tm)}$, and the rest of the submatrices are determined accordingly. Define the function for the matrix X :

$$\begin{aligned} \mathcal{A}_3(X) \\ = (X_{yz} - X_{y\phi} (X_{\phi\phi})^\dagger X_{\phi z}) (X_{zz} - X_{z\phi} (X_{\phi\phi})^\dagger X_{\phi z})^{-1}. \end{aligned}$$

It can be established that \mathcal{A}_3 is differentiable at \mathcal{W} , and that

$$Y_f^{(N)\perp} Z^{(N)\perp\dagger} = \mathcal{A}_3(\mathcal{W}^{(N)}), \quad \check{\eta}_{f,\infty} = \mathcal{A}_3(\mathcal{W}).$$

Further define $\tilde{\mathcal{A}}_3(X) = \mathcal{A}_3(X + \mathcal{W}) - \check{\eta}_{f,\infty}$, then $\tilde{\mathcal{A}}_3$ is differentiable at 0 and $\tilde{\mathcal{A}}_3(0) = 0$. Using Lemma 3.3 in [54],

$$\mathcal{A}_3(\mathcal{W}^{(N)} - \mathcal{W}) = \mathcal{A}_3(\mathcal{W}^{(N)}) - \check{\eta}_{f,\infty} \sim \mathcal{C}(-0.5).$$

The first equation in the lemma then follows after some calculations regarding $\mathcal{A}_3(\mathcal{W})$.

Next, we consider the simplification of $\Sigma_f^{(N)}$. It can be shown through matrix calculations that:

$$I - \Xi^{(N)\dagger} \Xi^{(N)} = (I - \Phi^{(N)\dagger} \Phi^{(N)}) (I - Z^{(N)\perp\dagger} Z^{(N)\perp}).$$

Thus, we have the simplification:

$$\begin{aligned} \Sigma_f^{(N)} &= \frac{1}{N} Y_f^{(N)\perp} (I - Z^{(N)\perp\dagger} Z^{(N)\perp}) \\ &\quad (I - Z^{(N)\perp\dagger} Z^{(N)\perp})^\top Y_f^{(N)\perp\top}. \end{aligned}$$

Based on this simplification, similar to the case of $\Theta_f^{(N)}$, an explicit relationship between $\Sigma_f^{(N)}$ and $\mathcal{W}^{(N)}$ can be

established (explicit expression omitted for brevity). We then define the function for the matrix X as follows:

$$\begin{aligned} \mathcal{A}_4(X) &= X_{yy} - X_{y\phi} (X_{\phi\phi})^\dagger X_{\phi y} \\ &\quad - (X_{yz} - X_{y\phi} (X_{\phi\phi})^\dagger X_{\phi z}) (X_{zz} - X_{z\phi} (X_{\phi\phi})^\dagger X_{\phi z})^{-1} \\ &\quad \cdot (X_{zy} - X_{z\phi} (X_{\phi\phi})^\dagger X_{\phi y}). \end{aligned}$$

It can be established that \mathcal{A}_4 is differentiable at \mathcal{W} , $\Sigma_f^{(N)} = \mathcal{A}_4(\mathcal{W}^{(N)})$ and $\check{\eta}_{f,\infty} = \mathcal{A}_4(\mathcal{W})$. Using Lemma 3.3 in [54], the second equation in the lemma follows. \square

C. Establishing the relationship between the limit and KF

We now prove by induction that the derived limit corresponds to the recursion of a KF (25). For brevity, we present the proof only for the single-trajectory case, as the multi-trajectory case follows similarly by replacing $\bar{\mathbb{E}}_t$ with \mathbb{E} . To establish this connection, we first introduce several notations. For the trajectory under consideration and $t = 2, 3, \dots$, define:

$$\begin{aligned} z_{t,ini}^- &= \text{col}(u_1, \dots, u_{t-1}, y_1, \dots, y_{t-1}), \\ z_{t,ini} &= \text{col}(u_1, \dots, u_{t-1}, y_1, \dots, y_t), \end{aligned}$$

and $z_{1,ini} = y_1$. Then, for the KF in (25) initialized by $\hat{x}_1^- = 0$, $P_1^- = \Sigma$, similar to (39), the predicted expectation of the KF can be simplified as:

$$\hat{x}_t^- = \hat{\theta}_t^-(\Sigma) z_{t,ini}^-, \quad \hat{x}_t = \hat{\theta}_t(\Sigma) z_{t,ini},$$

where both coefficients $\hat{\theta}_t^- : \mathbb{R}^{n \times n} \rightarrow \mathbb{R}^{n \times (t-1)(p+m)}$ and $\hat{\theta}_t : \mathbb{R}^{n \times n} \rightarrow \mathbb{R}^{n \times (t-1)(p+m)+p}$ are functions of Σ similar to the definition of $\hat{\theta}_{T_{ini}+1}^-$. We also define the covariance matrices P_t^- , P_t as functions of Σ similar to the definition of $P_{T_{ini}}^-$ in the main body of the paper.

On the other hand, define the following terms regarding the trajectory library as:

$$\begin{aligned} \tilde{z}_{t+l}^- &= \text{col}(\tilde{u}_{t+l-1}, \dots, \tilde{u}_t, \tilde{y}_t, \dots, \tilde{y}_{t+l-1}), \\ \tilde{z}_{t+l} &= \text{col}(\tilde{u}_{t+l-1}, \dots, \tilde{u}_t, \tilde{y}_t, \dots, \tilde{y}_{t+l}), \end{aligned}$$

with $l = 1, \dots, T_{ini}$ and $\tilde{z}_t = \tilde{y}_t$. Note that the ordering of the vectors u in this definition is slightly different from the main body of the paper, which necessitates the use of a permutation matrix later. Moreover, in the rest of this subsection, for a random vector h_{t+l} , $l = 0, 1, \dots$, define the operation

$$h_{t+l}^\perp = h_{t+l} - \bar{\mathbb{E}}_t(h_{t+l} \tilde{\phi}_t^\top) \bar{\mathbb{E}}_t(\tilde{\phi}_t \tilde{\phi}_t^\top)^\dagger \tilde{\phi}_t.$$

Next, define the coefficients $\tilde{\theta}_{l+1}^-$, $\tilde{\theta}_l$ as follows for $l = 1, \dots, T_{ini}$:

$$\begin{aligned} \tilde{\theta}_l &= \bar{\mathbb{E}}_t(\tilde{x}_{t+l-1}^\perp \tilde{z}_{t+l-1}^{\perp\top}) \bar{\mathbb{E}}_t(\tilde{z}_{t+l-1}^\perp \tilde{z}_{t+l-1}^{\perp\top})^{-1}, \\ \tilde{\theta}_{l+1}^- &= \bar{\mathbb{E}}_t(\tilde{x}_{t+l}^\perp \tilde{z}_{t+l}^{\perp\top}) \bar{\mathbb{E}}_t(\tilde{z}_{t+l}^{\perp\top} \tilde{z}_{t+l}^{\perp\top})^{-1}, \end{aligned}$$

Similarly, define the covariance matrices:

$$\begin{aligned} \tilde{P}_l &= \bar{\mathbb{E}}_t(\tilde{x}_{t+l-1}^\perp \tilde{z}_{t+l-1}^{\perp\top}) - \bar{\mathbb{E}}_t(\tilde{x}_{t+l-1}^\perp \tilde{z}_{t+l-1}^{\perp\top}) \\ &\quad \cdot \bar{\mathbb{E}}_t(\tilde{z}_{t+l-1}^\perp \tilde{z}_{t+l-1}^{\perp\top})^{-1} \bar{\mathbb{E}}_t(\tilde{z}_{t+l-1}^\perp \tilde{x}_{t+l-1}^{\perp\top}), \\ \tilde{P}_{l+1}^- &= \bar{\mathbb{E}}_t(\tilde{x}_{t+l}^\perp \tilde{z}_{t+l}^{\perp\top}) \\ &\quad - \bar{\mathbb{E}}_t(\tilde{x}_{t+l}^\perp \tilde{z}_{t+l}^{\perp\top}) \bar{\mathbb{E}}_t(\tilde{z}_{t+l}^{\perp\top} \tilde{z}_{t+l}^{\perp\top})^{-1} \bar{\mathbb{E}}_t(\tilde{z}_{t+l}^{\perp\top} \tilde{x}_{t+l}^{\perp\top}), \end{aligned}$$

Next, we prove by induction that:

$$\tilde{\theta}_l = \hat{\theta}_l(\Sigma) \mathcal{Q}_{l-1,l}, \quad \tilde{P}_l = P_l(\Sigma),$$

with $l = 1, \dots, T_{ini}$, where $\mathcal{Q}_{l,q}$ is a permutation matrix:

$$\mathcal{Q}_{l,q} = \begin{bmatrix} \mathcal{Q}_l & 0 \\ 0 & I_{pq} \end{bmatrix},$$

and Q_l is a permutation matrix:

$$\mathcal{Q}_l = [q_{ij}]_{l \times l} \otimes I_m, \quad q_{ij} = \begin{cases} 1 & \text{if } i + j \equiv l + 1 \\ 0 & \text{otherwise} \end{cases}.$$

This permutation arises from the different orderings of u in the definitions of \tilde{z}_{t+l} in this proof and in the main body.

Base case ($l = 1$): For $\Sigma = \bar{\mathbb{E}}_t(\tilde{x}_t^\perp \tilde{x}_t^{\perp\top})$, it follows that

$$\tilde{P}_1 = \Sigma - \Sigma C^\top (C \Sigma C^\top + R)^{-1} C \Sigma.$$

Moreover, according to the definition of \tilde{x}_t^\perp ,

$$\begin{aligned} \Sigma &= \bar{\mathbb{E}}_t(\tilde{x}_t^\perp \tilde{x}_t^{\perp\top}) = \bar{\mathbb{E}}_t(\tilde{x}_t \tilde{x}_t^\top) \\ &\quad - \bar{\mathbb{E}}_t(\tilde{x}_t \tilde{\phi}_t^\top) \bar{\mathbb{E}}_t(\tilde{\phi}_t \tilde{\phi}_t^\top)^\dagger \bar{\mathbb{E}}_t(\tilde{\phi}_t \tilde{x}_t^\top). \end{aligned} \quad (48)$$

Then, using the definition of $\bar{\mathbb{E}}_t$, we obtain that Σ matches the expression in Theorem 4.

Similarly, the expression of $\tilde{\theta}_1$ is:

$$\tilde{\theta}_1 = \Sigma C^\top (C \Sigma C^\top + R)^{-1}.$$

Hence, $\tilde{\theta}_1$ and \tilde{P}_1 correspond to the first measurement update step of the KF in (25).

Induction step: Assume the relations hold for some $l \geq 1$, we now prove that they hold for $l + 1$ using the following lemmas:

Lemma 13. *The terms \tilde{P}_l , \tilde{P}_{l+1}^- and $\tilde{\theta}_l$, $\tilde{\theta}_{l+1}^-$ have the following relationships respectively:*

$$\tilde{P}_{l+1}^- = A \tilde{P}_l A^\top + Q, \quad \tilde{\theta}_{l+1}^- = [B \quad A \tilde{\theta}_l].$$

Proof. We first consider the relationship between \tilde{P}_{l+1}^- and \tilde{P}_l . For simplicity of notation, let

$$\begin{aligned} \Gamma_{xx} &= \bar{\mathbb{E}}_t(\tilde{x}_{t+l-1}^\perp \tilde{x}_{t+l-1}^{\perp\top}), \quad \Gamma_{xz} = \Gamma_{zx}^\top = \bar{\mathbb{E}}_t(\tilde{x}_{t+l-1}^\perp \tilde{z}_{t+l-1}^{\perp\top}), \\ \Gamma_{zz} &= \bar{\mathbb{E}}_t(\tilde{z}_{t+l-1}^\perp \tilde{z}_{t+l-1}^{\perp\top}), \quad \Gamma_{xu} = \Gamma_{ux}^\top = \bar{\mathbb{E}}_t(\tilde{x}_{t+l-1}^\perp \tilde{u}_{t+l-1}^{\perp\top}), \\ \Gamma_{uu} &= \bar{\mathbb{E}}_t(\tilde{u}_{t+l-1}^\perp \tilde{u}_{t+l-1}^{\perp\top}). \end{aligned}$$

Based on these definitions, \tilde{P}_l and $\tilde{\theta}_l$ can be expressed as:

$$\tilde{P}_l = \Gamma_{xx} - \Gamma_{xz} \Gamma_{zz}^{-1} \Gamma_{zx}, \quad \tilde{\theta}_l = \Gamma_{xz} \Gamma_{zz}^{-1},$$

and

$$\begin{aligned} \bar{\mathbb{E}}_t(\tilde{x}_{t+l}^\perp \tilde{x}_{t+l}^{\perp\top}) &= A \Gamma_{xx} A^\top + A \Gamma_{xu} B^\top \\ &\quad + B \Gamma_{ux} A^\top + B \Gamma_{uu} B^\top + Q. \end{aligned}$$

Moreover, based on the definition of \tilde{z}_{t+l-1}^\perp and \tilde{z}_{t+l}^\perp :

$$\tilde{z}_{t+l}^\perp = \text{col}(\tilde{u}_{t+l-1}^\perp, \tilde{z}_{t+l-1}^\perp).$$

Hence,

$$\bar{\mathbb{E}}_t(\tilde{x}_{t+l}^\perp \tilde{z}_{t+l}^{\perp\top}) = [A \Gamma_{xz} + B \Gamma_{uz} \quad A \Gamma_{xu} + B \Gamma_{uu}], \quad (49)$$

$$\bar{\mathbb{E}}(\tilde{z}_{t+l}^\perp \tilde{z}_{t+l}^{\perp\top}) = \begin{bmatrix} \Gamma_{uu} & \Gamma_{uz} \\ \Gamma_{zu} & \Gamma_{zz} \end{bmatrix}.$$

Next, using block matrix inversion lemma to $\bar{\mathbb{E}}(\tilde{z}_{t+l}^\perp \tilde{z}_{t+l}^{\perp\top})$ and after algebraic manipulation, this yields

$$\tilde{P}_{l+1}^- = A \tilde{P}_l A^\top + Q + f(\Sigma_{xu} - \Sigma_{xz} \Sigma_{zz}^{-1} \Sigma_{zu}), \quad (50)$$

where $f(\Sigma_{xu} - \Sigma_{xz} \Sigma_{zz}^{-1} \Sigma_{zu})$ is a linear function of $\Sigma_{xu} - \Sigma_{xz} \Sigma_{zz}^{-1} \Sigma_{zu}$.

Notice that $\Sigma_{xz} \Sigma_{zz}^{-1} = \tilde{\theta}_l$. Then, the term can be expanded as:

$$\Sigma_{xu} - \Sigma_{xz} \Sigma_{zz}^{-1} \Sigma_{zu} = \bar{\mathbb{E}}_t((\tilde{x}_{t+l-1}^\perp - \tilde{\theta}_l \tilde{z}_{t+l-1}^\perp) \tilde{u}_{t+l-1}^{\perp\top}).$$

According to the definition of $\tilde{\theta}_l$, the following equation holds:

$$\bar{\mathbb{E}}_t((\tilde{x}_{t+l-1}^\perp - \tilde{\theta}_l \tilde{z}_{t+l-1}^\perp) \tilde{z}_{t+l-1}^{\perp\top}) = 0.$$

Moreover, according to the dynamics of the controller in Assumption 2, it follows that $\tilde{u}_{t+l-1} = \vartheta_1 \phi_t + \vartheta_2 \tilde{z}_{t+l-1} + \tilde{\nu}_{t+l-1}$, where ϑ_1 and ϑ_2 are appropriately dimensioned matrices that depend on the controller parameters. Then,

$$\begin{aligned} \tilde{u}_{t+l-1}^\perp &= \tilde{u}_{t+l-1} - \bar{\mathbb{E}}_t(\tilde{u}_{t+l-1} \tilde{\phi}_t^\top) \bar{\mathbb{E}}_t(\tilde{\phi}_t \tilde{\phi}_t^\top)^\dagger \tilde{\phi}_t \\ &= \vartheta_2 \tilde{z}_{t+l-1}^\perp + \tilde{\nu}_{t+l-1}. \end{aligned}$$

Hence,

$$\begin{aligned} \Sigma_{xu} - \Sigma_{xz} \Sigma_{zz}^{-1} \Sigma_{zu} &= \bar{\mathbb{E}}_t((\tilde{x}_{t+l-1}^\perp - \tilde{\theta}_l \tilde{z}_{t+l-1}^\perp) \tilde{z}_{t+l-1}^{\perp\top}) \vartheta_2^\top \\ &\quad + \bar{\mathbb{E}}_t((\tilde{x}_{t+l-1}^\perp - \tilde{\theta}_l \tilde{z}_{t+l-1}^\perp) \tilde{\nu}_{t+l-1}^\top) = 0. \end{aligned} \quad (51)$$

Then, combining the result above with (50), we obtain

$$\tilde{P}_{l+1}^- = A \tilde{P}_l A^\top + Q.$$

Moreover, combining the recursion in (49) with equation (51) yields

$$\begin{aligned} \bar{\mathbb{E}}_t(\tilde{x}_{t+l}^\perp \tilde{z}_{t+l}^{\perp\top}) \bar{\mathbb{E}}_t(\tilde{z}_{t+l}^\perp \tilde{z}_{t+l}^{\perp\top}) &= [B \quad A \Sigma_{xz} \Sigma_{zz}^{-1}] \\ &= [B \quad A \tilde{\theta}_l]. \end{aligned} \quad \square$$

Hence, Lemma 13 shows that the terms \tilde{P}_l , \tilde{P}_{l+1}^- , and $\tilde{\theta}_l \mathcal{Q}_{l+1,l}$, $\tilde{\theta}_{l+1}^- \mathcal{Q}_{l,l}$ align with a single time update step of the KF in (25).

Next, we introduce another lemma to address the measurement update step of the KF:

Lemma 14. *Let $\tilde{K}_l = \tilde{P}_l C^\top (C \tilde{P}_l C^\top + R)^{-1}$, then, the terms \tilde{P}_l^- , \tilde{P}_l and $\tilde{\theta}_l^-$ and $\tilde{\theta}_l$ are related as follows:*

$$\tilde{P}_l = (I - \tilde{K}_l C) \tilde{P}_l^-, \quad \tilde{\theta}_l^- = [(I - \tilde{K}_l C) \tilde{\theta}_l^- \quad \tilde{K}_l].$$

Proof. We first consider the relationship between \tilde{P}_l^- and \tilde{P}_l . For simplicity of notation, let

$$\begin{aligned} \Gamma_{xx} &= \bar{\mathbb{E}}_t(\tilde{x}_{t+l-1}^\perp \tilde{x}_{t+l-1}^{\perp\top}), \quad \Gamma_{xz} = \Gamma_{zx}^\top = \bar{\mathbb{E}}_t(\tilde{x}_{t+l-1}^\perp \tilde{z}_{t+l-1}^{\perp\top}), \\ \Gamma_{zz} &= \bar{\mathbb{E}}_t(\tilde{z}_{t+l-1}^\perp \tilde{z}_{t+l-1}^{\perp\top}), \quad \Gamma_{xu} = \Gamma_{ux}^\top = \bar{\mathbb{E}}_t(\tilde{x}_{t+l-1}^\perp \tilde{u}_{t+l-1}^{\perp\top}), \\ \Gamma_{uu} &= \bar{\mathbb{E}}_t(\tilde{u}_{t+l-1}^\perp \tilde{u}_{t+l-1}^{\perp\top}). \end{aligned}$$

Then,

$$\tilde{P}_l^- = \Gamma_{xx} - \Gamma_{xz} \Gamma_{zz}^{-1} \Gamma_{zx}, \quad \tilde{\theta}_l^- = \Gamma_{xz} \Gamma_{zz}^{-1}.$$

Notice that $\tilde{z}_{t+l-1}^\perp = \text{col}(\tilde{z}_{t+l-1}^\perp, \tilde{y}_{t+l-1}^\perp)$, it follows that

$$\bar{\mathbb{E}}_t(\tilde{x}_{t+l-1}^\perp \tilde{z}_{t+l-1}^{\perp\top}) = [\Gamma_{xz} \quad \Gamma_{xx} C^\top],$$

$$\bar{\mathbb{E}}_t(\tilde{z}_{t+l-1}^\perp \tilde{z}_{t+l-1}^{\perp\top}) = \begin{bmatrix} \Gamma_{zz} & \Gamma_{zx} C^\top \\ C\Gamma_{xz} & C\Gamma_{xx} C^\top + R \end{bmatrix}.$$

Then, using block matrix inversion lemma to $\bar{\mathbb{E}}_t(\tilde{z}_{t+l-1}^\perp \tilde{z}_{t+l-1}^{\perp\top})$ and by routine calculations, we arrive at

$$\tilde{P}_l = \tilde{P}_l^- - \tilde{P}_l^- C^\top F C \tilde{P}_l^-,$$

where $F = (C\Gamma_{xx} C^\top + R)^{-1}$. Similarly, it follows that

$$\tilde{\theta}_l = [\tilde{\theta}_l^- - \tilde{P}_l^- C^\top F \tilde{\theta}_l^- \quad \tilde{P}_l^- C^\top F],$$

Let $\tilde{K}_l = \tilde{P}_l^- C^\top F = \tilde{P}_l^- C^\top (C\tilde{P}_l^- C^\top + R)^{-1}$. Substituting this expression yields the desired identity and completes the proof. \square

From Lemma 14, it can be deduced that the relationships between \tilde{P}_l , \tilde{P}_l^- , and $\tilde{\theta}_l \mathcal{Q}_{l-1,l}$, $\tilde{\theta}_l^- \mathcal{Q}_{l-1,l-1}$ correspond to the measurement update step of the Kalman Filter.

Hence, by mathematical induction, we have established that:

$$\tilde{\theta}_l = \hat{\theta}_l(\Sigma) \mathcal{Q}_{l-1,l}, \quad \tilde{P}_l = P_l(\Sigma), l = 1, \dots, T_{ini}.$$

By applying Lemma 13, it can also be shown that:

$$\tilde{\theta}_l^- = \hat{\theta}_l^-(\Sigma) \mathcal{Q}_{l-1,l-1}, \quad \tilde{P}_l^- = P_l^-(\Sigma), l = 2, \dots, T_{ini} + 1.$$

Finally, let us examine the relationship between $\tilde{P}_{T_{ini}+1}^-$ and the asymptotic covariance $\tilde{\mathcal{Y}}_{f,\infty}$ in Lemma 12, as well as $\tilde{\theta}_{T_{ini}+1}^-$ and $\tilde{\eta}_{f,\infty}$. Define:

$$\tilde{z}_{t+T_{ini}+T}^\perp = \text{col}(\mathcal{Q}_{T_{ini}-1, T_{ini}} \tilde{z}_{t+T_{ini}}^\perp, \tilde{u}_f^\perp),$$

where $\tilde{u}_f = \text{col}(\tilde{u}_{t+T_{ini}}, \dots, \tilde{u}_{t+T_{ini}+T-1})$. Additionally, it follows that:

$$\tilde{y}_f^\perp = O_f \tilde{x}_{t+T_{ini}+1}^\perp + H_f \tilde{u}_f^\perp + G_f \tilde{w}_f + \tilde{v}_f,$$

where $\tilde{w}_f = \text{col}(\tilde{w}_{t+T_{ini}-1}, \dots, \tilde{w}_{t+T_{ini}+T-1})$, $\tilde{v}_f = \text{col}(\tilde{v}_{t+T_{ini}}, \dots, \tilde{v}_{t+T_{ini}+T})$. Using a similar technique as in the proof of Lemma 13, we obtain:

$$\begin{aligned} \tilde{\mathcal{Y}}_{f,\infty} &= O_f \tilde{P}_{T_{ini}+1}^- O_f^\top + G_f Q_f G_f^\top + R_f \\ &= O_f P_{T_{ini}+1}^-(\Sigma) O_f^\top + G_f Q_f G_f^\top + R_f, \\ \tilde{\eta}_{f,\infty} &= [O_f \mathcal{Q}_{T_{ini}-1, T_{ini}} \tilde{\theta}_{T_{ini}+1}^- H_f] = [O_f \tilde{\theta}_{T_{ini}+1}^-(\Sigma) H_f]. \end{aligned}$$

Thus, the statements of Theorem 4 have been fully proven. Moreover, since the proof of Theorem 4 and the proof of Theorem 6 in Appendix III does not rely on any Gaussian assumptions, Proposition 8 can also be established using the same proofs.

APPENDIX III PROOF OF THEOREM 6

Proof. The gap between the two distributions considered in Theorem 6 is equivalent to the gap between the following two distributions:

- The estimation of $x_{T_{ini}+1}$ using T_{ini} initial samples, as discussed in Theorem 4. This estimation is the output of a KF that takes the past T_{ini} samples as inputs, initialized with $(0, \Sigma)$.
- The estimation of $x_{T_{ini}+1}$ using all available past samples, as described in Proposition 5. This estimation is the output of a KF that takes all past samples as inputs, initialized with (μ_T, Σ_T) .

For both KFs, we consider the time interval from $t = 1$ to $t = T_{ini}$. During this interval, both filters share the same state-space parameters and input-output samples, with the only difference being the initial distribution of x_1 , which is $(0, \Sigma)$ for the first filter and (\hat{x}_1^-, P_1^-) for the second.

Hence, as $T_{ini} \rightarrow \infty$, applying Lemma 15 proves the theorem. \square

Lemma 15 (Stability of KF with respect to its initialization). *For the LTI system (1), suppose (A, C) is detectable and $(A, Q^{1/2})$ is stabilizable. Let $\hat{x}_{t,11}^-, P_{t,1}^-$ and $\hat{x}_{t,22}^-, P_{t,2}^-$ denote the output of the Kalman filter recursively updated by the same I/O samples, but initialized by two different conditions (μ_1, Σ_1) and (μ_2, Σ_2) as in (25). Then, there exists $0 < \rho < 1$, such that*

$$\lim_{t \rightarrow \infty} \|P_{t,1}^- - P_{t,2}^-\| \rho^{-t} = 0, \quad \lim_{t \rightarrow \infty} \|\hat{x}_{t,11}^- - \hat{x}_{t,22}^-\| \rho^{-t} = 0 \text{ a.s.}$$

Proof. First, due to the assumptions in the lemma, we know from [38, Chapter 4], [55] that for any initialization of the covariance in the Kalman filter, there exists a constant $\Phi > 0$, such that

$$\|P_t^- - P^*\| \leq \Phi \rho^t,$$

where $\rho = \rho(A - AK^*C) < 1$, $\rho(X)$ denotes the spectral radius of the matrix X and P^* is the unique positive definite solution to the Riccati equation:

$$P^* = AP^*A^\top - AP^*C^\top(CP^*C^\top + R)^{-1}CP^*A^\top + Q.$$

Hence, we can conclude that for any $\underline{\rho} < \rho < 1$,

$$\lim_{t \rightarrow \infty} \|P_{t,1}^- - P^*\| \rho^{-t} = 0, \quad \lim_{t \rightarrow \infty} \|P_{t,2}^- - P^*\| \rho^{-t} = 0.$$

Therefore,

$$\begin{aligned} 0 &\leq \limsup_{t \rightarrow \infty} \|P_{t,1}^- - P_{t,2}^-\| \rho^{-t} \\ &\leq \lim_{t \rightarrow \infty} \|P_{t,1}^- - P^*\| \rho^{-t} + \lim_{t \rightarrow \infty} \|P_{t,2}^- - P^*\| \rho^{-t} = 0. \end{aligned} \tag{52}$$

We next consider the second equation in the lemma. Let the corresponding Kalman gain of $P_{t,1}^-$ and $P_{t,2}^-$ be $K_{t,1}$ and $K_{t,2}$ respectively. Since

$$K_{t,*} = P_{t,*}^- C^\top (CP_{t,*}^- C^\top + R)^{-1},$$

where $*$ can be either 1 or 2, we bound the difference between $K_{t,1}$ and $K_{t,2}$ as:

$$\begin{aligned} & K_{t,1} - K_{t,2} \\ &= P_{t,1}^- C^\top (CP_{t,1}^- C^\top + R)^{-1} - P_{t,2}^- C^\top (CP_{t,1}^- C^\top + R)^{-1} \\ &\quad + P_{t,2}^- C^\top (CP_{t,1}^- C^\top + R)^{-1} - P_{t,2}^- C^\top (CP_{t,2}^- C^\top + R)^{-1}. \end{aligned} \quad (53)$$

The difference between the first two terms in the equation above are bounded by the difference between $P_{t,1}^-$ and $P_{t,2}^-$. It remains to bound the difference between the last two terms. Let $S_{1,t} = CP_{t,1}^- C^\top + R$, $S_{2,t} = CP_{t,2}^- C^\top + R$, and $E_t = C(P_{t,1}^- - P_{t,2}^-)C^\top$. Then

$$\|S_{1,t}^{-1} - S_{2,t}^{-1}\| \leq \|S_{1,t}^{-1}\| \|S_{2,t}^{-1}\| \|E_t\|.$$

Since $R \succ 0$, both $S_{1,t}$ and $S_{2,t}$ are uniformly positive definite, and thus $\|S_{1,t}^{-1}\| \|S_{2,t}^{-1}\| \leq \tilde{\Phi}$ for some constant $\tilde{\Phi} > 0$. Hence, combining the boundedness above with (52) and (53), for all $\underline{\rho} < \rho < 1$,

$$\lim_{t \rightarrow \infty} \|K_{t,1} - K_{t,2}\| \rho^{-t} = 0. \quad (54)$$

Now, we are ready to consider the difference between $\hat{x}_{t,11}^-$ and $\hat{x}_{t,22}^-$, which can be derived as:

$$\begin{aligned} \hat{x}_{t,11}^- - \hat{x}_{t,22}^- &= (A - AK_{t-1,1}C)\hat{x}_{t-1,11}^- \\ &\quad + AK_{t-1,1}y_{t-1} - (A - AK_{t-1,2}C)\hat{x}_{t-1,22}^- - AK_{t-1,2}y_{t-1}. \end{aligned}$$

Let $\chi_t = \hat{x}_{t,11}^- - \hat{x}_{t,22}^-$ and let $\tilde{K}_t = K_{t,1} - K_{t,2}$. It follows that

$$\begin{aligned} \chi_t &= \hat{x}_{t,11}^- - \hat{x}_{t,22}^- \\ &= \underbrace{(A - AK_{t-1,1}C)}_{\tilde{A}_{t-1}} \chi_{t-1} + \underbrace{AK_{t-1}(y_{t-1} - C\hat{x}_{t-1,22}^-)}_{\epsilon_{t-1}}. \end{aligned} \quad (55)$$

For a sufficiently large t , consider the following common Lyapunov function:

$$V(\chi_t) = \chi_t^\top P^* \chi_t.$$

Then, using the recursion in (55),

$$V(\chi_{t+1}) = \chi_t^\top \tilde{A}_t^\top P^* \tilde{A}_t \chi_t + \Gamma_{t+1},$$

where

$$\begin{aligned} \Gamma_{t+1} &= \chi_t^\top \tilde{A}_t^\top P^* A \tilde{K}_t \epsilon_t + \epsilon_t^\top \tilde{K}_t^\top A^\top P^* \tilde{A}_t \chi_t \\ &\quad + \epsilon_t^\top \tilde{K}_t^\top A^\top P^* A \tilde{K}_t \epsilon_t. \end{aligned} \quad (56)$$

Hence, let $\tilde{A} = (A - AK^*C)$,

$$\begin{aligned} V(\chi_{t+1}) - V(\chi_t) &= \chi_t^\top (\tilde{A}^\top P^* \tilde{A} - P^*) \chi_t \\ &\quad + \chi_t^\top (\tilde{A}_t^\top P^* \tilde{A}_t - \tilde{A}^\top P^* \tilde{A}) \chi_t + \Gamma_{t+1}. \end{aligned}$$

Notice that P^* satisfies:

$$P^* = \tilde{A}^\top P^* \tilde{A} + A^\top K^{*\top} R K^* A + Q,$$

it can be deduced that

$$\begin{aligned} V(\chi_{t+1}) - V(\chi_t) &= -\chi_t^\top (A^\top K^{*\top} R K^* A + Q) \chi_t \\ &\quad + \chi_t^\top (\tilde{A}_t^\top P^* \tilde{A}_t - \tilde{A}^\top P^* \tilde{A}) \chi_t + \Gamma_{t+1}. \end{aligned} \quad (57)$$

According to (54), there exists constants $L_1, L_2, L_3 > 0$, such that

$$\|\tilde{A}_t^\top P^* \tilde{A}_t - \tilde{A}^\top P^* \tilde{A}\| \leq L_1 \rho^t,$$

$$|\Gamma_{t+1}| \leq L_2 \|\chi_t\| \rho^t + L_3 \rho^{2t} \text{ a.s.},$$

for all $\underline{\rho} < \rho < 1$. Let $\eta = \lambda_{\min}(A^\top K^{*\top} R K^* A + Q) > 0$. Then, for a fixed $\rho \in (\underline{\rho}, 1)$, there exists constants $L > 0$, $\underline{\eta} > 0$ and a time index $T_1 > 0$, such that for all $t \geq T_1$,

$$\eta - L_1 \rho^t - \frac{L_2 L + L_3}{L^2} \geq \underline{\eta} > 0.$$

Suppose there exists $t \geq T_1$, such that $\|\chi_t\| \geq L \rho^t$. Otherwise, the proposition is already proved. Then,

$$\begin{aligned} V(\chi_{t+1}) - V(\chi_t) &\leq -\|\chi_t\|^2 (\eta - L_1 \rho^t) + |\Gamma_{t+1}| \\ &\leq -\|\chi_t\|^2 (\eta - L_1 \rho^t) + \left(\frac{L_2 L + L_3}{L^2} \right) \|\chi_t\|^2 \\ &\leq -\underline{\eta} \|\chi_t\|^2 \leq -\frac{\eta}{\|P^*\|} V(\chi_t) \text{ a.s.} \end{aligned} \quad (58)$$

Moreover, we can verify through the definition of η that $0 < \underline{\eta}/\|P^*\| < 1$. Hence, we can prove the exponentially convergence of $\|\chi_t\|$ to 0 for all $t \geq T_1$, as long as $\|\chi_t\| \geq L \rho^t$. Then, we can conclude that there exists constants $\rho < 1$, $L_4 > 0$, such that for all $t \geq T_1$,

$$\|\chi_t\| \leq L_4 \rho^t. \quad (59)$$

Hence, we can prove the second equation in the lemma. \square

APPENDIX IV PROOF OF REMARK 5

Theorem 16. Suppose the assumptions in Section II hold, and let

$$r \triangleq n_{\text{ctrl}} + m(T_{\text{ini}} + T) + pT_{\text{ini}}$$

denote the number of rows of $\Xi^{(N)}$. If $N \geq r(T_{\text{ini}} + T + \kappa_{\text{ctrl}}) + 1$, then $\Xi^{(N)}$ has full row rank almost surely, i.e.,

$$\mathbb{P}(\text{rank } \Xi^{(N)} = r) = 1,$$

whenever the noise process satisfies one of the following conditions:

- (i) the Gaussian noise model in Section II;
- (ii) the non-Gaussian model in Assumption 4.

Proof. We first consider the case where the system noise is Gaussian and the trajectory library is constructed from a single trajectory. Recall that we assume that $v_t \sim \mathcal{N}(0, R)$ and $\nu_t \sim \mathcal{N}(0, R_{\text{ctrl}})$ with $R \succ 0$, $R_{\text{ctrl}} \succ 0$, mutually independent and independent of initial conditions and plant process noise. The controller $(A_{\text{ctrl}}, B_{\text{ctrl}}, C_{\text{ctrl}})$ is a minimal realization; let n_{ctrl} be its state dimension and κ_{ctrl} the controllability index of $(A_{\text{ctrl}}, B_{\text{ctrl}})$. Recall that $K = T_{\text{ini}} + T + N - 1$ denotes the length of the single trajectory in \mathcal{D} .

In this proof, we aim to show that $\Xi^{(N)}$ has full row rank almost surely. Since its row dimension is r , it suffices to show that one can extract r linearly independent columns. Our strategy is as follows: Part I develops a universal triangular

factorization for fixed (u, y) -windows. Part II extends this factorization by propagating the noise terms through the controller, thereby obtaining a decomposition of the combined vector formed by (ϕ, u, y) , which constitutes columns of $\Xi^{(N)}$. Part III selects r columns of $\Xi^{(N)}$ and concatenates them into a global block-lower-triangular map to establish that the selected submatrix is nonsingular. Finally, Part IV concludes almost-sure full row rank of $\Xi^{(N)}$ via an algebraic-variety and absolute-continuity argument.

Define

$$\tilde{x}_t = \text{col}(x_t, y_t, \phi_t, u_t), \quad \tilde{y}_t = \text{col}(u_t, y_t),$$

and the augmented system

$$\begin{aligned}\tilde{x}_{t+1} &= \tilde{A}\tilde{x}_t + \tilde{w}_t + \tilde{G}\tilde{v}_t, \\ \tilde{y}_t &= \tilde{C}\tilde{x}_t,\end{aligned}$$

where

$$\begin{aligned}\tilde{w}_t &= \begin{bmatrix} w_t \\ Cw_t \\ 0 \\ 0 \end{bmatrix}, \quad \tilde{v}_t = \begin{bmatrix} \nu_t \\ v_t \end{bmatrix}, \quad \tilde{C} = \begin{bmatrix} 0 & 0 & 0 & I \\ 0 & I & 0 & 0 \end{bmatrix}, \\ \tilde{G} &= \begin{bmatrix} 0 & 0 \\ 0 & I \\ 0 & 0 \\ I & 0 \end{bmatrix}, \quad \tilde{A} = \begin{bmatrix} A & 0 & 0 & B \\ CA & 0 & 0 & CB \\ 0 & B_{\text{ctrl}} & A_{\text{ctrl}} & 0 \\ 0 & C_{\text{ctrl}}B_{\text{ctrl}} & C_{\text{ctrl}}A_{\text{ctrl}} & 0 \end{bmatrix}.\end{aligned}$$

A direct calculation gives $\tilde{C}\tilde{G} = \text{diag}(I, I)$.

Part I: Triangular factorization for (u, y) -windows.
Stack $\tilde{y}_{1:K}^d$:

$$\tilde{y}_{1:K}^d = \tilde{O}_K \tilde{x}_0^d + \tilde{G}_K \tilde{w}_{0:K-1}^d + \tilde{G}_K(I_K \otimes \tilde{G}) \tilde{v}_{0:K-1}^d,$$

where

$$\tilde{O}_K = \begin{bmatrix} \tilde{C}\tilde{A} \\ \tilde{C}\tilde{A}^2 \\ \vdots \\ \tilde{C}\tilde{A}^K \end{bmatrix}, \quad \tilde{G}_K = \begin{bmatrix} \tilde{C} & 0 & \cdots & 0 \\ \tilde{C}\tilde{A} & \tilde{C} & \cdots & 0 \\ \vdots & \vdots & \ddots & \vdots \\ \tilde{C}\tilde{A}^{K-1} & \tilde{C}\tilde{A}^{K-2} & \cdots & \tilde{C} \end{bmatrix}.$$

Since $\tilde{C}\tilde{G} = I$, the matrix $\tilde{G}_K(I_K \otimes \tilde{G})$ is block lower triangular with identity diagonal blocks and hence invertible.

Let $\tilde{\mathcal{Q}} = [I \ 0]$ so that $\tilde{\mathcal{Q}}\tilde{y}_t^d = u_t^d$. Define the fixed selection (reordering) operator

$$\tilde{\mathcal{Q}}_{-T:-1} = \begin{bmatrix} I & 0 \\ 0 & (I_T \otimes \tilde{\mathcal{Q}}) \end{bmatrix},$$

$$\zeta \triangleq \text{col}(\tilde{y}_{1:T_{\text{ini}}+N-1}^d, u_{T_{\text{ini}}+N:K}^d).$$

Then

$$\begin{aligned}\zeta &= \tilde{\mathcal{Q}}_{-T:-1} \tilde{y}_{1:K}^d = \underbrace{\tilde{\mathcal{Q}}_{-T:-1} \tilde{O}_K \tilde{x}_0^d + \tilde{\mathcal{Q}}_{-T:-1} \tilde{G}_K \tilde{w}_{0:K-1}^d}_{\rho_\zeta} \\ &\quad + \underbrace{\tilde{\mathcal{Q}}_{-T:-1} \tilde{G}_K(I_K \otimes \tilde{G}) \tilde{v}_{0:K-1}^d}_{\mathbf{T}_\zeta}.\end{aligned}$$

Here \mathbf{T}_ζ is obtained from a block lower-triangular, unit-diagonal matrix by deleting matched rows/columns; thus

it remains block lower triangular with unit diagonal and is invertible. Since ρ_ζ is independent of $\tilde{v}_{0:K-1}^d$ and $\text{Cov}(\tilde{v}_{0:K-1}^d) = \text{diag}(I \otimes R_{\text{ctrl}}, I \otimes R) \succ 0$,

$$\text{Cov}(\zeta) = \text{Cov}(\rho_\zeta) + \mathbf{T}_\zeta \text{Cov}(\tilde{v}_{0:K-1}^d) \mathbf{T}_\zeta^\top \succ 0.$$

Using this proof, any (u, y) -stack extracted from $\tilde{y}_{1:K}^d$ by a fixed selection admits a representation “independent term + invertible lower-triangular map \times Gaussian noise” and is nondegenerate Gaussian.

Part II: Controller propagation and single-column decomposition of $\Xi^{(N)}$. Based on the factorization in Part I, we now exploit the factorization of a specific column of $\Xi^{(N)}$.

(i) The first column with ϕ_1 . Consider the first column $\mathbf{c}^{(1)} = \text{col}(\phi_1^d, u_{1:T_{\text{ini}}+T}^d, y_{1:T_{\text{ini}}}^d)$. Define

$$\boldsymbol{\eta}^{(1)} = \text{col}(\phi_1^d, v_{1:T_{\text{ini}}+T}^d, v_{1:T_{\text{ini}}}^d),$$

and write

$$\mathbf{c}^{(1)} = \rho^{(1)} + \mathbf{T}^{(1)} \boldsymbol{\eta}^{(1)}, \quad \mathbf{T}^{(1)} = \begin{bmatrix} I_{n_{\text{ctrl}}} & 0 & 0 \\ * & \mathsf{L}_u^{(1)} & 0 \\ * & * & \mathsf{L}_y^{(1)} \end{bmatrix}.$$

Here $\rho^{(1)}$ is independent of $\boldsymbol{\eta}^{(1)}$; the blocks $\mathsf{L}_u^{(1)}, \mathsf{L}_y^{(1)}$ are unit-diagonal lower-triangular (from Part I). Since $\text{Cov}(\phi_1) \succ 0$ and $R_{\text{ctrl}}, R \succ 0$, $\text{Cov}(\boldsymbol{\eta}^{(1)}) \succ 0$ and $\mathbf{T}^{(1)}$ has full row rank, so $\mathbf{c}^{(1)}$ is nondegenerate Gaussian.

(ii) Noise-only factorization of the y -window and its injection into ϕ . Fix $s \geq 0$. By the triangular factorization in Part I, any fixed y -window admits

$$y_{s+1:s+\kappa_{\text{ctrl}}} = \underbrace{\rho_y^{(s)}}_{\text{independent of } v_{s+1:s+\kappa_{\text{ctrl}}}} + \underbrace{T_y^{(s)}}_{\substack{\text{block lower triangular} \\ \text{unit diagonal}}} v_{s+1:s+\kappa_{\text{ctrl}}}.$$

Unrolling the controller over κ_{ctrl} steps and injecting the above decomposition yields

$$\begin{aligned}& \phi_{s+\kappa_{\text{ctrl}}+1} \\ &= \underbrace{A_{\text{ctrl}}^{\kappa_{\text{ctrl}}} \phi_{s+1} + \mathcal{C}_{\text{ctrl}} \rho_y^{(s)} + \zeta_s + \mathcal{C}_{\text{ctrl}} T_y^{(s)} v_{s+1:s+\kappa_{\text{ctrl}}}}_{\rho_\phi^{(s)} \perp v_{s+1:s+\kappa_{\text{ctrl}}}} + \underbrace{\tilde{T}_\phi^{(s)}}_{\tilde{T}_\phi^{(s)}}\end{aligned}$$

where $\mathcal{C}_{\text{ctrl}} \in \mathbb{R}^{n_{\text{ctrl}} \times (p\kappa_{\text{ctrl}})}$ denotes the κ_{ctrl} -step controllability matrix of the stabilizing controller:

$$\mathcal{C}_{\text{ctrl}} = [A_{\text{ctrl}}^{\kappa_{\text{ctrl}}-1} B_{\text{ctrl}} \ A_{\text{ctrl}}^{\kappa_{\text{ctrl}}-2} B_{\text{ctrl}} \ \cdots \ B_{\text{ctrl}}],$$

$\tilde{T}_\phi^{(s)}$ is a fixed block lower-triangular map (and has full row rank n_{ctrl} by controllability of $(A_{\text{ctrl}}, B_{\text{ctrl}})$), $\rho_\phi^{(s)}$ is independent of $v_{s+1:s+\kappa_{\text{ctrl}}}$, and ζ_s collects state and noise terms up to time s .

Since $(A_{\text{ctrl}}, B_{\text{ctrl}})$ is controllable and κ_{ctrl} is its controllability index, this block row has full row rank n_{ctrl} . Moreover, $T_y^{(s)}$ is invertible; hence $\tilde{T}_\phi^{(s)}$ also has full row rank.

Therefore, there exists an index set $\mathcal{J} \subset \{1, \dots, p\kappa_{\text{ctrl}}\}$ with $|\mathcal{J}| = n_{\text{ctrl}}$ such that the square submatrix

$$\hat{\mathcal{C}}^{(s)} \triangleq (\tilde{T}_\phi^{(s)})_{:, \mathcal{J}} \in \mathbb{R}^{n_{\text{ctrl}} \times n_{\text{ctrl}}}$$

is nonsingular. As a result, the s -column $\mathbf{c}^{(s)}$ of $\Xi^{(N)}$ admits the following decomposition:

$$\mathbf{c}^{(s)} = \boldsymbol{\rho}^{(s)} + \mathbf{T}^{(s)}\boldsymbol{\eta}^{(s)}, \quad (60)$$

where

$$\boldsymbol{\rho}^{(s)} = \text{col}(\rho_\phi^{(s)}, \rho_y^{(s)}),$$

$$\boldsymbol{\eta}^{(s)} = \text{col}(v_{s-\kappa_{\text{ctrl}}:s-1}, v_{s:s+T_{\text{ini}}+T-1}, v_{s:s+T_{\text{ini}}-1}),$$

with the block-lower-triangular structure

$$\mathbf{T}^{(s)} = \begin{bmatrix} \hat{\mathcal{C}}^{(s)} & 0 & 0 \\ * & \mathsf{L}_u^{(s)} & 0 \\ * & * & \mathsf{L}_y^{(s)} \end{bmatrix},$$

where $\hat{\mathcal{C}}^{(s)}$ is invertible, and $\mathsf{L}_u^{(s)}, \mathsf{L}_y^{(s)}$ are unit-diagonal lower-triangular. Hence, $\mathbf{T}^{(s)}$ is invertible.

Part III: Column selection and block-lower-triangular concatenation. Next, we are ready to introduce how to construct the r columns to be picked. We set the start times at

$$t_1 \triangleq 1, \quad t_k \triangleq k(T_{\text{ini}} + T + \kappa_{\text{ctrl}}) + 1, \quad k = 2, \dots, r,$$

so that each picked column uses the blocks $\phi_{t_k}, u_{t_k:t_k+T_{\text{ini}}+T-1}, y_{t_k:t_k+T_{\text{ini}}-1}$.

We now stack the r selected columns together:

$$\boldsymbol{\eta}_{\text{all}} = \text{col}(\boldsymbol{\eta}^{(1)}, \dots, \boldsymbol{\eta}^{(r)}), \quad \boldsymbol{\rho}_{\text{all}} = \text{col}(\boldsymbol{\rho}^{(1)}, \dots, \boldsymbol{\rho}^{(r)}),$$

and the column stack

$$\mathbf{C} = \text{col}(\mathbf{c}^{(1)}, \dots, \mathbf{c}^{(r)}) = \boldsymbol{\rho}_{\text{all}} + \mathbf{T}_{\text{big}}\boldsymbol{\eta}_{\text{all}},$$

where

$$\mathbf{T}_{\text{big}} = \begin{bmatrix} \mathsf{T}^{(1)} & 0 & \cdots & 0 \\ *_{21} & \mathsf{T}^{(2)} & \cdots & 0 \\ \vdots & \ddots & \ddots & \vdots \\ *_{r1} & \cdots & *_{r,r-1} & \mathsf{T}^{(r)} \end{bmatrix}$$

is *block lower triangular* with *diagonal blocks* $\mathsf{T}^{(j)}$. The starred blocks capture causal overlaps but do not destroy triangularity. Since each $\mathsf{T}^{(j)}$ is nonsingular, \mathbf{T}_{big} is also nonsingular. Moreover $\text{Cov}(\boldsymbol{\eta}_{\text{all}}) \succ 0$ because each component of $\boldsymbol{\eta}^{(j)}$ is drawn from nondegenerate Gaussians (ϕ_1, ν, v) . Therefore

$$\text{Cov}(\mathbf{C}) = \text{Cov}(\boldsymbol{\rho}_{\text{all}}) + \mathbf{T}_{\text{big}}\text{Cov}(\boldsymbol{\eta}_{\text{all}})\mathbf{T}_{\text{big}}^\top \succ 0.$$

Part IV: Algebraic-variety step and almost-sure full row rank.

Let

$$\boldsymbol{\zeta}_{\text{all}} \triangleq \text{col}\left(\phi_{t_k}, u_{t_k:t_k+T_{\text{ini}}+T-1}, y_{t_k:t_k+T_{\text{ini}}-1}\right)_{k=1}^r$$

denote the stacked random vector on which \mathbf{C} depends (so we may write $\mathbf{C} = \mathbf{C}(\boldsymbol{\zeta}_{\text{all}})$). Set

$$\Delta(\boldsymbol{\zeta}_{\text{all}}) = \det(\mathbf{C}).$$

Then Δ is a polynomial in the entries of $\boldsymbol{\zeta}_{\text{all}}$, and

$$\{\text{rank } \Xi^{(N)} < r\} \subseteq \{\Delta(\boldsymbol{\zeta}_{\text{all}}) = 0\}.$$

By our column construction, each entry of \mathbf{C} depends on a *distinct* scalar coordinate of $\boldsymbol{\zeta}_{\text{all}}$. Hence these entries can be prescribed independently. In particular, choose a deterministic point $\boldsymbol{\zeta}_{\text{all}}^*$ such that $\mathbf{C}(\boldsymbol{\zeta}_{\text{all}}^*) = I_r$; then $\Delta(\mathbf{C}(\boldsymbol{\zeta}_{\text{all}}^*)) = 1 \neq 0$, so Δ is not the zero polynomial.

Therefore, the set

$$\mathcal{M} = \{\boldsymbol{\zeta}_{\text{all}} : \Delta(\boldsymbol{\zeta}_{\text{all}}) = 0\} \subset \mathbb{R}^{r^2}$$

is an algebraic variety of Lebesgue measure zero. Let λ denote Lebesgue measure on \mathbb{R}^{r^2} and let μ be the measure induced by $\boldsymbol{\zeta}_{\text{all}}$. By construction, $\boldsymbol{\zeta}_{\text{all}}$ is jointly Gaussian with a nonsingular covariance matrix; hence μ admits an everywhere positive density with respect to λ , i.e., $\mu \ll \lambda$. Consequently every λ -null set is also μ -null, and since $\lambda(\mathcal{M}) = 0$ we have $\mu(\mathcal{M}) = 0$.

Thus the rank-deficiency event has probability zero, i.e.,

$$\mathbb{P}(\text{rank } \Xi^{(N)} = r) = 1.$$

Moreover, when the trajectory library consists of multiple independent trajectories, Assumption 3 ensures that the random vectors forming each column of $\Xi^{(N)}$ are jointly Gaussian with a nonsingular covariance matrix. Applying the same argument as above, we again conclude that $\Xi^{(N)}$ has full row rank almost surely.

Non-Gaussian extension. The argument above did not rely on any particular Gaussian property beyond absolute continuity with respect to the Lebesgue measure. Hence the almost-sure full row rank conclusion extends to a broader class of noise distributions.

For the case where the trajectory library is constructed from a single trajectory, recall that $\mathbf{C} = \boldsymbol{\rho}_{\text{all}} + \mathbf{T}_{\text{big}}\boldsymbol{\eta}_{\text{all}}$, where \mathbf{T}_{big} is block lower triangular with full row rank and thus invertible. By Assumption 4, the support of $\boldsymbol{\eta}_{\text{all}}$ has nonempty interior. Then, by invertibility of \mathbf{T}_{big} , the support of $\boldsymbol{\zeta}_{\text{all}}$ also has nonempty interior. Consequently, the measure induced by $\boldsymbol{\zeta}_{\text{all}}$ is absolutely continuous with respect to Lebesgue measure. Since the rank-deficiency event is contained in the algebraic variety \mathcal{M} which has Lebesgue measure zero, it follows that $\mathbb{P}(\mathcal{M}) = 0$. Therefore,

$$\mathbb{P}(\text{rank } \Xi^{(N)} = r) = 1.$$

The same argument applies when the trajectory library consists of multiple independent trajectories, completing the proof. \square

REFERENCES

- [1] M. Morari and J. H. Lee, “Model predictive control: past, present and future,” *Computers & Chemical Engineering*, vol. 23, no. 4, pp. 667–682, 1999.
- [2] A. Bemporad and M. Morari, “Robust model predictive control: A survey,” in *Robustness in identification and control* (A. Garulli and A. Tesi, eds.), (London), pp. 207–226, Springer London, 1999.

- [3] G. Mahalakshmi, S. Sridevi, and S. Rajaram, "A survey on forecasting of time series data," in *2016 international conference on computing technologies and intelligent data engineering (ICCTIDE'16)*, pp. 1–8, IEEE, 2016.
- [4] R. Isermann, "Model-based fault-detection and diagnosis—status and applications," *Annual Reviews in control*, vol. 29, no. 1, pp. 71–85, 2005.
- [5] V. Venkatasubramanian, R. Rengaswamy, K. Yin, and S. N. Kavuri, "A review of process fault detection and diagnosis: Part i: Quantitative model-based methods," *Computers & chemical engineering*, vol. 27, no. 3, pp. 293–311, 2003.
- [6] E. Kaufmann, L. Bauersfeld, A. Loquercio, M. Müller, V. Koltun, and D. Scaramuzza, "Champion-level drone racing using deep reinforcement learning," *Nature*, vol. 620, no. 7976, pp. 982–987, 2023.
- [7] M. Neunert, M. Stäuble, M. Gifthaler, C. D. Bellicos, J. Carius, C. Gehring, M. Hutter, and J. Buchli, "Whole-body nonlinear model predictive control through contacts for quadrupeds," *IEEE Robotics and Automation Letters*, vol. 3, no. 3, pp. 1458–1465, 2018.
- [8] J. C. Knight, "Safety critical systems: challenges and directions," in *Proceedings of the 24th international conference on software engineering*, pp. 547–550, 2002.
- [9] J. Coulson, J. Lygeros, and F. Dörfler, "Data-enabled predictive control: In the shallows of the deepc," in *2019 18th European Control Conference (ECC)*, pp. 307–312, IEEE, 2019.
- [10] J. Coulson, J. Lygeros, and F. Dörfler, "Distributionally robust chance constrained data-enabled predictive control," *IEEE Transactions on Automatic Control*, vol. 67, no. 7, pp. 3289–3304, 2022.
- [11] L. Ljung, "System identification," in *Signal analysis and prediction*, pp. 163–173, Springer, 1998.
- [12] B. HO and R. E. Kálmán, "Effective construction of linear state-variable models from input/output functions," *ar-Automaticsierungstechnik*, vol. 14, no. 1-12, pp. 545–548, 1966.
- [13] P. Van Overschee and B. De Moor, "N4sid: Subspace algorithms for the identification of combined deterministic-stochastic systems," *Automatica*, vol. 30, no. 1, pp. 75–93, 1994. Special issue on statistical signal processing and control.
- [14] M. Verhaegen, "Identification of the deterministic part of mimo state space models given in innovations form from input-output data," *Automatica*, vol. 30, no. 1, pp. 61–74, 1994. Special issue on statistical signal processing and control.
- [15] P. Verheijen, V. Breschi, and M. Lazar, "Handbook of linear data-driven predictive control: Theory, implementation and design," *Annual Reviews in Control*, vol. 56, p. 100914, 2023.
- [16] F. Dorfler, J. Coulson, and I. Markovsky, "Bridging Direct and Indirect Data-Driven Control Formulations via Regularizations and Relaxations," *IEEE Transactions on Automatic Control*, vol. 68, pp. 883–897, Feb. 2023.
- [17] M. Sader, Y. Wang, D. Huang, C. Shang, and B. Huang, "Causality-informed data-driven predictive control," *IEEE Transactions on Control Systems Technology*, pp. 1–8, 2025.
- [18] Y. Wang, K. You, D. Huang, and C. Shang, "Data-driven output prediction and control of stochastic systems: An innovation-based approach," *Automatica*, vol. 171, p. 111897, 2025.
- [19] I. Markovsky and F. Dörfler, "Behavioral systems theory in data-driven analysis, signal processing, and control," *Annual Reviews in Control*, vol. 52, pp. 42–64, 2021.
- [20] J. Willems, P. Rapisarda, I. Markovsky, and B. De Moor, "A note on persistency of excitation," *Systems and Control Letters*, vol. 54(4), 04 2005.
- [21] P. Mattsson and T. B. Schön, "On the regularization in deepc*," *IFAC-PapersOnLine*, vol. 56, no. 2, pp. 625–631, 2023. 22nd IFAC World Congress.
- [22] G. Pan, R. Ou, and T. Faulwasser, "On a Stochastic Fundamental Lemma and Its Use for Data-Driven Optimal Control," *IEEE Transactions on Automatic Control*, vol. 68, pp. 5922–5937, Oct. 2023. arXiv:2111.13636 [cs, eess, math].
- [23] G. Pan, R. Ou, and T. Faulwasser, "Towards data-driven stochastic predictive control," *International Journal of Robust and Nonlinear Control*, 2023.
- [24] S. Kerz, J. Teutsch, T. Brüdigam, D. Wollherr, and M. Leibold, "Data-driven tube-based stochastic predictive control," *arXiv preprint*, 2023. arXiv:2112.04439.
- [25] J. Teutsch, S. Kerz, D. Wollherr, and M. Leibold, "Sampling-based stochastic data-driven predictive control under data uncertainty," *arXiv preprint*, 2024. arXiv:2402.00681.
- [26] H. Kwakernaak, "Robust control and h_∞ optimization—tutorial paper," *Automatica*, vol. 29, no. 2, pp. 255–273, 1993.
- [27] M. Mirza, "Conditional generative adversarial nets," *arXiv preprint*, 2014. arXiv:1411.1784.
- [28] K. Sohn, H. Lee, and X. Yan, "Learning structured output representation using deep conditional generative models," *Advances in neural information processing systems*, vol. 28, 2015.
- [29] A. Ajay, Y. Du, A. Gupta, J. Tenenbaum, T. Jaakkola, and P. Agrawal, "Is conditional generative modeling all you need for decision-making?," *arXiv preprint*, 2022. arXiv:2211.15657.
- [30] Y. Song, J. Sohl-Dickstein, D. P. Kingma, A. Kumar, S. Ermon, and B. Poole, "Score-based generative modeling through stochastic differential equations," *International Conference on Learning Representations*, 2021.
- [31] Y. Lipman, R. T. Q. Chen, H. Ben-Hamu, M. Nickel, and M. Le, "Flow matching for generative modeling," *International Conference on Learning Representations*, 2023.
- [32] K. L. Chung, *A course in probability theory*. Elsevier, 2000.
- [33] T. Faulwasser, R. Ou, G. Pan, P. Schmitz, and K. Worthmann, "Behavioral theory for stochastic systems? A data-driven journey from Willems to Wiener and back again," *Annual Reviews in Control*, vol. 55, pp. 92–117, 2023.
- [34] M. Klädtke and M. S. Darup, "Towards explainable data-driven predictive control with regularizations," *arXiv preprint*, 2025. arXiv:2503.21952.
- [35] L. Ljung, *Practical issues of system identification*. Linköping University Electronic Press, 2007.
- [36] P. S. Heuberger, P. M. Van den Hof, and B. Wahlberg, *Modelling and Identification with Rational Orthogonal Basis Functions*. 2005.
- [37] P. V. d. Hof, B. Wahlberg, P. Heuberger, B. Ninness, J. Bokor, and T. O. e. Silva, "Modelling and Identification with Rational Orthogonal Basis Functions," *IFAC Proceedings Volumes*, vol. 33, no. 15, pp. 445–455, 2000.
- [38] B. D. Anderson and J. B. Moore, *Optimal filtering*. Courier Corporation, 2005.
- [39] J. Elfring, E. Torta, and R. van de Molengraft, "Particle filters: A hands-on tutorial," *Sensors (Basel, Switzerland)*, vol. 21, 2021.
- [40] J. Humphreys, P. Redd, and J. West, "A fresh look at the kalman filter," *SIAM Review*, vol. 54, no. 4, pp. 801–823, 2012.
- [41] G. Schildbach, L. Fagiano, C. Frei, and M. Morari, "The scenario approach for Stochastic Model Predictive Control with bounds on closed-loop constraint violations," *Automatica*, vol. 50, pp. 3009–3018, Dec. 2014.
- [42] R. Li, J. W. Simpson-Porco, and S. L. Smith, "Stochastic data-driven predictive control with equivalence to stochastic mpc," *arXiv preprint*, 2023. arXiv:2312.15177.
- [43] P. J. Campo and M. Morari, "Robust model predictive control," in *1987 American Control Conference*, pp. 1021–1026, 1987.
- [44] C. M. Bishop, *Pattern recognition and machine learning*. Springer, 2006.
- [45] W. Favoreel, B. D. Moor, and M. Gevers, "Spc: Subspace predictive control," *IFAC Proceedings Volumes*, vol. 32, no. 2, pp. 4004–4009, 1999. 14th IFAC World Congress 1999, Beijing, China, 5–9 July.
- [46] H. Hjalmarsson, S. Gunnarsson, and M. Gevers, "Model-free tuning of a robust regulator for a flexible transmission system," *European Journal of Control*, vol. 1, no. 2, pp. 148–156, 1995.
- [47] I. Landau, D. Rey, A. Karimi, A. Voda, and A. Franco, "A flexible transmission system as a benchmark for robust digital control*," *European Journal of Control*, vol. 1, no. 2, pp. 77–96, 1995.
- [48] M. Campi, A. Lecchini, and S. Savarese, "Virtual reference feedback tuning: a direct method for the design of feedback controllers," *Automatica*, vol. 38, no. 8, pp. 1337–1346, 2002.
- [49] S. Oymak and N. Ozay, "Revisiting Ho–Kalman-Based System Identification: Robustness and Finite-Sample Analysis," *IEEE Transactions on Automatic Control*, vol. 67, pp. 1914–1928, Apr. 2022.
- [50] V. Breschi, A. Chiuso, and S. Formentin, "Data-driven predictive control in a stochastic setting: A unified framework," *Automatica*, vol. 152, p. 110961, 2023.
- [51] R. Dinkla, S. Mulders, T. Oomen, and J.-W. van Wingerden, "Closed-loop Data-Enabled Predictive Control and its equivalence with Closed-loop Subspace Predictive Control," Feb. 2024. arXiv:2402.14374 [cs, eess].
- [52] A. Chiuso and G. Picci, "On the ill-conditioning of subspace identification with inputs," *Automatica*, vol. 40, pp. 575–589, Apr. 2004.

- [53] J. Li, S. Sun, and Y. Mo, "Fundamental limit on siso system identification," in *2022 IEEE 61st Conference on Decision and Control (CDC)*, pp. 856–861, 2022.
- [54] H. Liu, Y. Mo, J. Yan, L. Xie, and K. H. Johansson, "An online approach to physical watermark design," *IEEE Transactions on Automatic Control*, vol. 65, no. 9, pp. 3895–3902, 2020.
- [55] D. Ocone and E. Pardoux, "Asymptotic stability of the optimal filter with respect to its initial condition," *SIAM Journal on Control and Optimization*, vol. 34, no. 1, pp. 226–243, 1996.

Jiayun Li received her Bachelor of Engineering degree from Department of Automation, Tsinghua University in 2022. She is currently a Ph.D. candidate in the Department of Automation, Tsinghua University. Her research interests include system identification, learning-based control.

Yilin Mo is an Associate Professor in the Department of Automation, Tsinghua University. He received his Ph.D. in Electrical and Computer Engineering from Carnegie Mellon University in 2012 and his Bachelor of Engineering degree from Department of Automation, Tsinghua University in 2007. Prior to his current position, he was a postdoctoral scholar at Carnegie Mellon University in 2013 and California Institute of Technology from 2013 to 2015. He held an assistant professor position in the School of Electrical and Electronic Engineering at Nanyang Technological University from 2015 to 2018. His research interests include secure control systems and networked control systems, with applications in sensor networks and power grids.